

**Grain-size variability of point-bar deposits from a fine-grained dryland river terminus, Southern Altiplano, Bolivia**

Li, Jiaguang; Vandenberghe, Jef; Mountney, Nigel P.; Luthi, Stefan M.

**DOI**

[10.1016/j.sedgeo.2020.105663](https://doi.org/10.1016/j.sedgeo.2020.105663)

**Publication date**

2020

**Document Version**

Final published version

**Published in**

Sedimentary Geology

**Citation (APA)**

Li, J., Vandenberghe, J., Mountney, N. P., & Luthi, S. M. (2020). Grain-size variability of point-bar deposits from a fine-grained dryland river terminus, Southern Altiplano, Bolivia. *Sedimentary Geology*, 403, 1-17. Article 105663. <https://doi.org/10.1016/j.sedgeo.2020.105663>

**Important note**

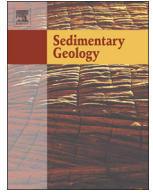
To cite this publication, please use the final published version (if applicable). Please check the document version above.

**Copyright**

Other than for strictly personal use, it is not permitted to download, forward or distribute the text or part of it, without the consent of the author(s) and/or copyright holder(s), unless the work is under an open content license such as Creative Commons.

**Takedown policy**

Please contact us and provide details if you believe this document breaches copyrights. We will remove access to the work immediately and investigate your claim.



# Grain-size variability of point-bar deposits from a fine-grained dryland river terminus, Southern Altiplano, Bolivia

Jianguang Li <sup>a,\*</sup>, Jef Vandenberghe <sup>b</sup>, Nigel P. Mountney <sup>c</sup>, Stefan M. Luthi <sup>d</sup>

<sup>a</sup> Key Laboratory of Tectonics and Petroleum Resources (China University of Geosciences), Ministry of Education, Wuhan 430074, China

<sup>b</sup> Faculty of Science, Vrije Universiteit Amsterdam, Amsterdam, the Netherlands

<sup>c</sup> School of Earth and Environment, University of Leeds, Leeds LS2 9JT, UK

<sup>d</sup> Department of Geoscience and Engineering, Delft University of Technology, Delft 2628 CN, the Netherlands

## ARTICLE INFO

### Article history:

Received 13 January 2020

Received in revised form 30 March 2020

Accepted 3 April 2020

Available online 8 April 2020

Editor: Dr. Catherine Chagué

### Keywords:

Semi-arid endorheic basin

Fine-grained

River terminus

Meandering river

Point bar

Coarsening-upward succession

## ABSTRACT

Point-bar deposits exhibiting fining-upward grain-size trends are widely documented from both modern rivers and ancient preserved successions. However, in some mud-dominated sedimentary systems this common pattern may not occur; rather, alternative coarsening-upward trends can develop. We investigated point-bar deposits in the mud-dominated river terminus (median value ( $D_{50}$ ) < 55  $\mu\text{m}$ ) of the meandering Río Colorado in Bolivia's southern Altiplano, a semi-arid endorheic basin. Grain-size trends were investigated using double random grain-size distribution (GSD) measurements and end-member modelling analyses (EMMA), as well as detailed mineralogical analyses (XRD and LOI). These methods revealed an upward-coarsening trend of point-bar deposits in terms of  $D_{50}$  of GSD and in proportions of coarse sediment for two (C2 and C0) of three chronologically different meandering channels in the river terminus. Those of another abandoned channel (C1) were, by contrast, dominated by a fining-upward trend. The deposits in channel C2 were characterised by a lower content of organic matter and carbonate compared with those of the other two channels. A novel conceptual model for the formation of coarsening-upward point-bar deposits is proposed. The model implies the action of low-frequency, high-magnitude floods during an overall hyper-arid period when sediment supply to the river terminus is dominated by clay and fine silt. A temporal trend toward higher magnitude and longer duration flood events allows for the transport coarser-grained sediments further down system toward the river terminus where deposition occurs on the inner bend of meandering channels. Successive accretion layers within the point-bar deposits record a coarsening upward trend. Results demonstrate how a coarsening-upward succession of point-bar deposits in the muddy river terminus of a semi-arid endorheic basin can contribute to improved understanding of mechanisms of deposition in fine-grained fluvial systems. Our results contribute to an improved understanding of the varied processes and sedimentology of very fine-grained meandering river terminus systems in semi-arid or arid endorheic basins; the results additionally provide insight to enable improved interpretations of rock record examples of pre-vegetation rivers on Earth and other planetary bodies.

© 2020 Elsevier B.V. All rights reserved.

## 1. Introduction

Point-bar deposits are a fundamental architectural element of meandering river systems (Miall, 1988; Colombera et al., 2013). Many point-bar elements comprise sand-prone deposits (Jackson, 1981; Thomas et al., 1987; Miall, 1988; Rygel and Gibling, 2006; Simon and Gibling, 2017a), and these can be economically important in subsurface successions where they serve to form groundwater aquifers and

hydrocarbon reservoirs (e.g., Smith et al., 2009; Donselaar et al., 2017a). Although highly variable with respect to their internal facies arrangement (e.g., Yan et al., 2017; Shiers et al., 2019), point-bar deposits commonly exhibit a fining-upward trend, with a coarse sand or gravel basal lag overlain by sand deposits that transition upward to fine sediments (silt and clay) (Bridge et al., 1995; Colombera and Mountney, 2019). This common fining-upward trend arises as a result of the gradual lateral shift of the channel pool – which hosts the strongest current in the channel – as it progressively moves outward in response to meander migration (Visher, 1964; Allen, 1963; Jackson, 1976; Nanson, 1980). Sand-prone point-bar deposits are commonly overlain directly by fine-grained floodplain sediments (Allen, 1963; Jackson, 1976; Nanson,

\* Corresponding author.

E-mail addresses: [jianguanglicn@yahoo.com](mailto:jianguanglicn@yahoo.com), [jianguangli@gmail.com](mailto:jianguangli@gmail.com) (J. Li).

1980). This fining-upward succession is common because the helicoidal flow regime present around a meander bend gradually loses momentum along the point-bar slope due to friction (Allen, 1963).

Recent studies note that different processes may operate in rivers that transport dominantly fine-grained sediment: in mud-dominated meandering river systems, sand- and silt-sized aggregates can be transported as bed load and be deposited along the flanks for growing point bars in sinuous channels; high smectite contents associated with vertisol-type soils appear to promote this (Maroulis and Nanson, 1996; Gibling et al., 1998; Wakelin-King and Webb, 2007; Simon and Gibling, 2017a, 2017b). According to these studies, cycles of wetting and drying can form mud aggregates with low densities, which are entrained, transported and deposited directly during flood events. The integrity of such sand-sized mud aggregates (also named “clay pellets”) may not necessarily be preserved during compaction. However, Müller et al. (2004) suggest that burial depth – and, by extension, compaction – does not seem to be an important factor for preservation of mud aggregates. The above-mentioned studies considered examples either from the rock record (e.g., the Triassic Lunde Formation Norway, Müller et al., 2004; the Lower Permian Clear Fork Formation of north-central Texas, USA, Simon and Gibling, 2017a, 2017b) or from the middle or upper reaches of point bars in recent fluvial systems (e.g., central Australia, Maroulis and Nanson, 1996; Gibling et al., 1998).

Sediments deposited in the terminal areas of large, low-gradient, dryland rivers tend to have been transported relatively long distances from upland source regions. In the distal parts of many such terminal rivers, silt- and clay-sized sediment dominates (Knighton, 1980; Ferguson et al., 1996; Rice and Church, 1998; Frings, 2008; Kemp, 2010). Coarser sediments are more common in the proximal piedmont area and in medial areas (Li et al., 2015). In semi-arid endorheic basins, this downstream pattern in particle size is attributed to the ephemerality of flow, characterised by infrequent and short-lived flash floods (Tooth, 2000; Li et al., 2015). Such systems commonly experience floods driven mostly by thunderstorm events (Knighton and Nanson, 2001; Alexandrov et al., 2003). These types of floods are not necessarily capable of transporting coarse-grained sediments along the entire river system (Graf, 1988; Nanson et al., 2002), likely because of a combination of (i) extremely low gradient in the distal regions of the fluvial plain (ii) the short duration of peak discharge events, with a rapid rising and falling stage; (iii) water loss due to infiltration and surface evaporation (Tooth, 2000; Donselaar et al., 2013). However, if the magnitudes and frequencies of floods increase, coarse sediments have a greater potential to be transported further downstream and may be deposited at the river terminus which, in endorheic basins, is the final depocentre, or the sediment sink. However, for fluvial systems in arid and semi-arid settings, prediction of the relationship between mean annual precipitation and sediment yield is not straightforward: in some systems, flood events are commonly of relatively low frequency but high magnitude and might be associated with high sediment yield for a given discharge event; in other systems, at the transition from an arid to a semi-arid climate regime the colonisation of the land surface by vegetation may act to retard surface runoff and sediment yield (Micheli and Kirchner, 2002; Comiti et al., 2011; Camacho Suarez et al., 2015). Furthermore, longer duration peak discharge events may entail longer transport distances of coarser sediment, thereby increasing the proportions of bedload deposited in the distal regions. Such trends in grain size are therefore thought to have the potential to help decipher subtle signals of climate changes in the tectonically quiescent regions (Coronel et al., 2020).

Here we investigate sediment dispersal and grain-size characteristics of point-bar deposits in the distal parts of a non-vegetated, fine-grained (median value ( $D_{50}$ ) < 55  $\mu\text{m}$ ) meandering river system, the Río Colorado terminus in the Salar de Uyuni in Bolivia's southern

Altiplano. The aim of this study is to develop a model to account for the origin of coarsening-upward point-bar deposits in a modern meandering river terminus in a semi- and arid endorheic basin through an investigation of the grain-size characteristics of point-bar successions that are dominated by clay and silt deposits with little to no sand. Specific research objectives are as follows: (i) to demonstrate how sediment samples collected from boreholes that penetrate point bars of palaeo-channels and active channels can be examined using a laser particle sizer for granulometric analysis as part of flume-based experiments to determine modes of sediment transport; (ii) to relate grain-size characters and mineralogy using a laser-diffraction particle sizer and X-ray diffraction (XRD) technique; (iii) to show how end-member modelling of the grain-size distribution can be applied to accurately quantify the proportions of the different components within the point-bar deposits; (iv) to develop a conceptual sedimentological model to demonstrate the formative processes of upward coarsening trend of point-bar deposits in the river terminus system of an endorheic system.

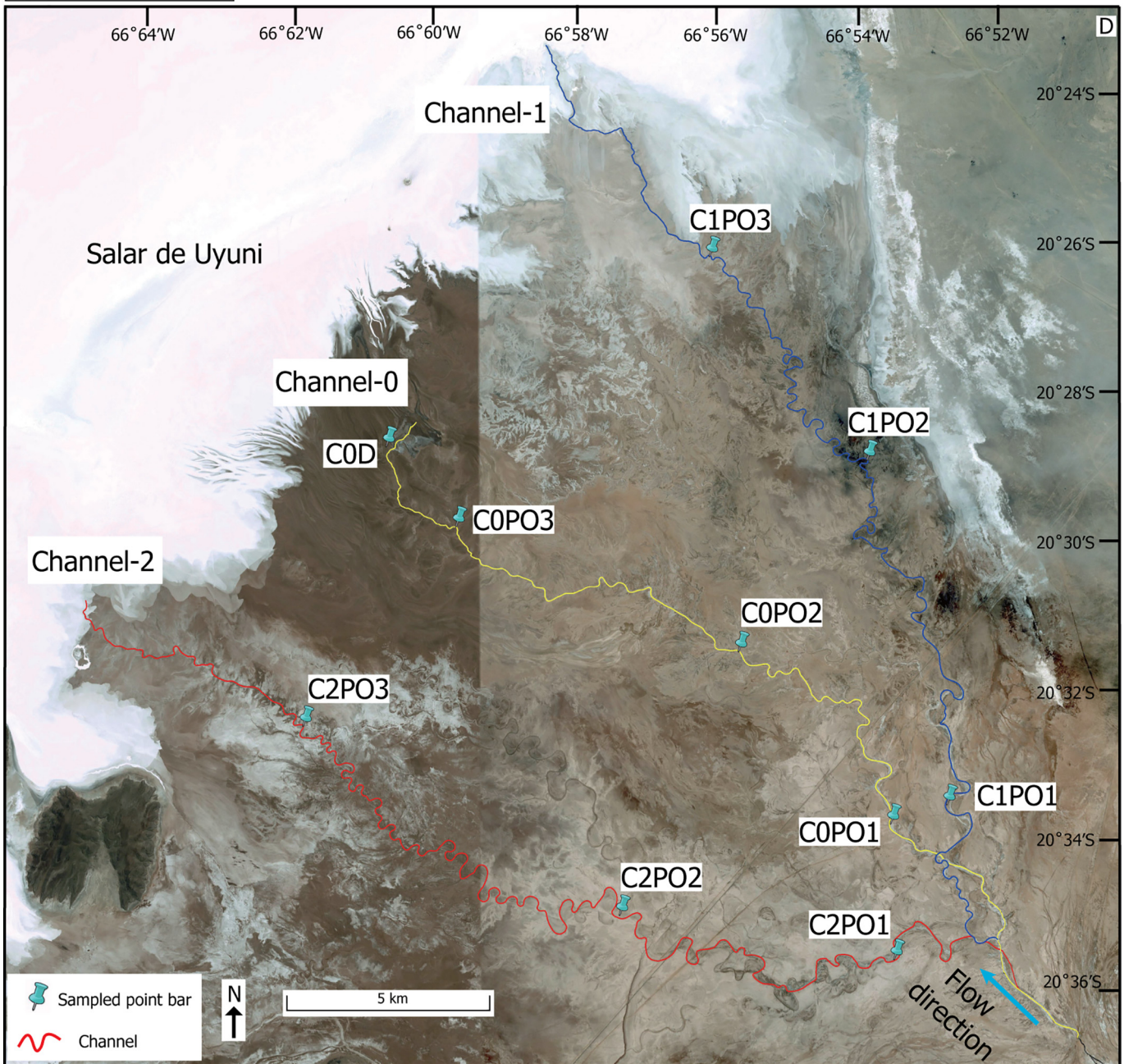
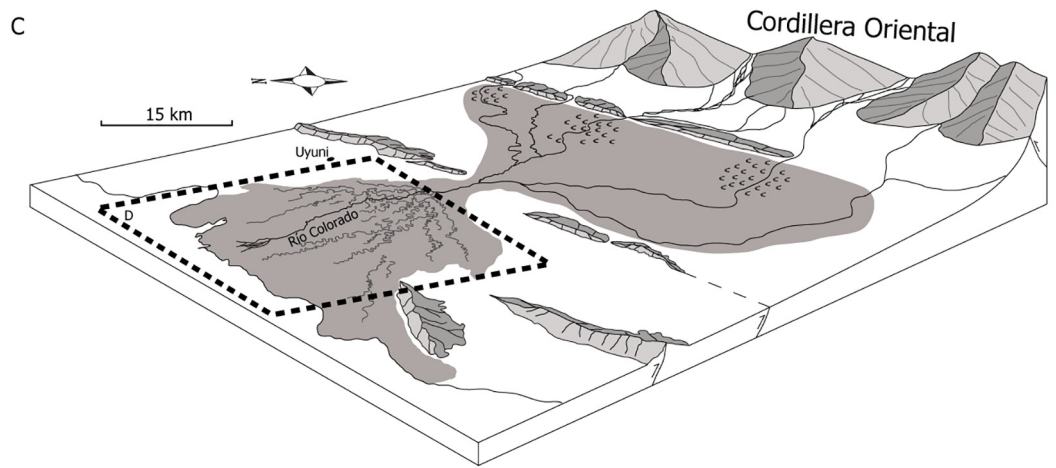
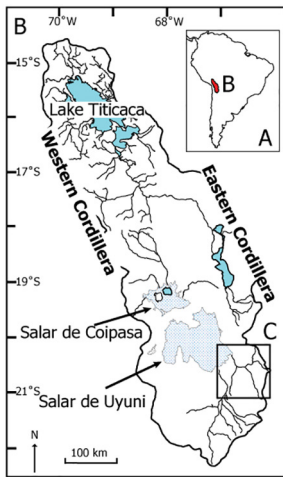
The results of this work have important implications for feasibility of granulometric analysis in fine-grained ( $D_{50}$  < 55  $\mu\text{m}$ ) meandering river termini, especially those in semi-arid and arid endorheic basin settings. Moreover, the results contribute toward an improved understanding of the variety of processes that govern the development of present-day non-vegetated meanders (e.g., Ielpi, 2018; Santos et al., 2019). Importantly, results may also inform on the growing appreciation of the apparent commonness of meandering river deposition on ‘pre-vegetation’ Earth and in the drivers of such styles of sedimentation (Marconato et al., 2014; Santos et al., 2017; McMahon and Davies, 2018; Ielpi et al., 2019).

## 2. Study area

The Altiplano Basin is an internally drained basin filled with Tertiary and Quaternary alluvial, lacustrine and volcanoclastic deposits (Fig. 1A, B, C) (Horton et al., 2001; Elger et al., 2005). Currently, the basin experiences a semi-arid climate with an annual precipitation of >800 mm in the north and <200 mm in the south (Argollo and Mourguiart, 2000) but the annual evapo-transpiration potential of 1500 mm greatly exceeds these precipitation ranges (Grosjean, 1994; Risacher et al., 2009). Three hydrographic regions can be distinguished in the Altiplano basin: the permanent Lake Titicaca, the seasonal hypersaline Lake Poopó, and the Salars (salt pans) of Coipasa and Uyuni. Sedimentological research employing various proxies (e.g. content of pollen and diatoms, composition of stromatolites and bioherms) revealed that the Altiplano basin has experienced oscillations of wet-dry climatic periods since the late Pleistocene. Boreholes in the southern Salar de Uyuni revealed a sediment record of alternating mud-salt layers in the lake centre in support of this (Bills et al., 1994; Sylvestre et al., 1995; Baker et al., 2001; Rigsby et al., 2005; Placzek et al., 2006).

The Río Colorado river terminus covers a non-vegetated area of ~475 km<sup>2</sup>. Sedimentological field studies have shown that this river terminus has deposited alluvium atop lacustrine muds that were deposited during a lake-level highstand period, though without significant fluvial channel incision due to a low topographic gradient and the action of ephemeral flows with low stream power (Donselaar et al., 2013). Geophysical and altimetric studies suggest the river terminus system has been tectonically quiescent in the late Pleistocene and Holocene (Bills et al., 1994; Baucom and Rigsby, 1999; Rigsby et al., 2005). The lower Río Colorado terminus is characterised by an overall low gradient: the maximum slope is  $5.75 \times 10^{-4}$ , declining to  $\sim 1.48 \times 10^{-5}$  (Li et al., 2015).

**Fig. 1.** Map of the study area. A) Location of the Altiplano Plateau in South America; B) and C) Site of the study area in the Altiplano plateau. D) Río Colorado terminus system and investigated channels on a Google Earth map. The flow direction is from upper right to lower left in C and from low right to upper left in D. A and B are modified after Placzek et al. (2011).



Optical stimulated luminescence (OSL) dating results have suggested that the overlying fluvial deposits formed after  $4.26 \pm 0.36$  ka (Donselaar et al., 2017b). Short-term analyses based on time-series satellite imagery have revealed a time-averaged frequency of channel avulsion of approximately five years in the distal part of the Río Colorado river terminus (Li et al., 2014a; Li and Bristow, 2015). An OSL-based long-term analysis of the proximal part of the river terminus indicated the frequency of nodal avulsion was approximately 200 years with a range from 60 to 910 years (Donselaar et al., 2017b). The channel switching in the proximal part of the river terminus systems is referred to as nodal avulsions, whereas avulsions in the distal part of the fan are so-called local avulsions (Slingerland and Smith, 2004). Different temporal scales of avulsion frequency indicate variations in the spatial effects of compensational stacking processes (e.g., Straub et al., 2009). Dates obtained from point-bar surfaces suggest multiple channels were abandoned from 3.64 ka to 0.70 ka, clustering into five age brackets (see Fig. 3 in Donselaar et al., 2017b).

The Río Colorado is characterised by seasonal activation and downstream reduction in cross-section area due to the coupled effects of low precipitation, strong evapo-transpiration and infiltration (Donselaar et al., 2013; Li et al., 2014a). Previous studies in this river terminus system have revealed prominent splay morphodynamics and sediment dispersal patterns (Li et al., 2014a, 2015, 2019, 2020; Li and Bristow, 2015; van Toorenburg et al., 2018). Low-frequency but high-magnitude floods have impacted considerably on the geomorphology and sedimentology of the river terminus, in particular in the distal part and floodplain of the river terminus due to significant overbank flooding (Li et al., 2018, 2019). However, a suite of multi-decadal satellite imagery also indicates that along the sinuous reaches of the present main channel no chute channels have developed (Li et al., 2019).

### 3. Data acquisition and methods

#### 3.1. Data acquisition

A two-week field campaign was conducted during the end of the dry period (Nov. 2012) and focused on sediment sampling of point-bar deposits along two palaeo-channels and the presently active channel. Additionally, other sedimentary elements such as crevasse splays, natural levees and floodplain deposits were investigated, the aim being to better understand the sedimentary and petrographic architecture of the Río Colorado river terminus. A total of 219 sediment samples were collected from the whole river terminus for further laboratory analysis: 90 from point-bar deposits; 58 from crevasse-splay deposits; 71 from floodplain deposits. These sediment samples were processed for grain-size distribution, the results of which have been used as input for endmember modelling (see below).

This paper focuses on the point bars of three channels, which emanated from the same parent channel at a point of nodal avulsion in the proximal part of the fluvial system, to traverse different parts of the fluvial lower plain (Fig. 1D). Combined with visual interpretation on Google Earth™ imagery of cross-cutting relationships and OSL dating results by Donselaar et al. (2017b), the three channels were chronologically numbered as C2 (1.1–0.9 ka), C1 (0.7–0.5 ka) and C0 (0.4 ka–present), respectively (Fig. 1D). Nine point-bars from proximal, medial and distal reaches were selected along these three channels. One additional point bar at the downstream end of channel C0 was additionally examined for validation of sedimentary responses to decadal scale changes in discharge (see text below).

Point-bar deposits directly downstream from sites of nodal avulsions in the proximal part of the river terminus are important, since the sedimentation of these point bars takes place during the active period of development of the channel prior to the occurrence of an avulsion event. Therefore, these deposits record the entire episode of evolution for the given channel. In contrast, point-bar deposits in

more distal settings are representative of only part of the active period due to high-frequency localised avulsion events in the downstream reaches of the channel in the river terminus. Prior studies have shown that the distal reaches of the main channel experienced multiple avulsions while the upstream reaches of the same channel remained stable (Li et al., 2014a, 2014b). For each of the three channels examined, three point bars located at exponentially greater distances downstream from the nodal point of the river terminus were numbered from 1 to 3. For each point bar, one borehole was dug for further analyses. For example, boreholes for each of the proximal, medial and distal reaches of channel 2 (C2) were labelled C2PO1, C2PO2 and C2PO3, respectively (Fig. 1D). Additionally, sediment sampling in another trench (C0D) was undertaken to investigate the response of sedimentation patterns in the Río Colorado terminus to changes in magnitude of precipitation (see below). For each examined point bar, differences in grain size and changes in the nature of salt cementation across lateral accretion surfaces enabled the identification of scroll-bar units in the field. This means that the surface expression of these scroll-bar units is evident on high-resolution satellite imagery, despite low topographic relief (Fig. 2A, B) (Donselaar et al., 2013). Following the identification of lateral accretion surfaces indicative of individually accreted scroll units, trenches were dug in the outermost three scroll units of each studied point bar (Fig. 2A, C). Direct field measurement of the presently active channel C0, reveals that the channel depth is <2 m and mostly between 1 m and 1.5 m, although a clear downstream reduction was observed (Donselaar et al., 2013). The trenches in the point-bar deposits adjacent to the edge of the channels were dug to a depth of 1 m. This is sufficiently deep to cover multiple accretional layers for characterisation of the vertical trend of point-bar deposits. The sediment sampling was performed using a shovel at intervals of 0.1 m or 0.2 m vertically (Fig. 2D, E). These trenches and laquer peels were also used to characterise the sedimentary structures (Fig. 2F).

All sampling locations were determined by cross-referencing to high-resolution satellite imagery on Google Earth™ for mapping purposes and using a GPS Garmin 60CSx in the field. The stated horizontal accuracy of the hand-held GPS is 3 to 5 m. Across the low-relief, unvegetated plateau at an altitude >3650 m, the GPS was tested to be accurate to 3 m (based on reference to fixed objects of known location).

Along with bi-temporal high-resolution satellite imagery (2005 and 2016) from Google Earth Pro™ and precipitation data from the Bolivian Servicio Nacional de Meteorología e Hidrología in the study area, the tenth borehole at the end of channel C0 was used to investigate the response of sedimentation patterns in the Río Colorado terminus to decadal scale changes in the magnitude of precipitation.

#### 3.2. Analytical methods

##### 3.2.1. Grain-size analysis and end-member modelling analysis (EMMA)

The Río Colorado terminus system is dominated by silt and clay (Li et al., 2015). To test the validity of grain-size distribution analysis using a laser-diffraction particle sizer, which assumes sediment is transported as single particles, a simple laboratory experiment was designed to examine sediment dispersal and to test the appropriateness of using the laser-based instrument. Before the grain-size analysis, sediment dispersal of the samples was qualitatively tested using randomly selected samples (nine samples in total). After naturally drying the samples through exposure to air, aggregates with different sizes (Fig. 3) in natural condition were subjected to two hydraulic conditions: (i) by simply adding sediment samples to beakers containing still deionised water (Fig. 3A–E); (ii) by adding sediment samples to beakers first and then slowly adding deionised water into the beakers (Fig. 3F–J). Water temperature was 25 °C. Timing was set to quantify the rate of sediment dispersal processes from angular aggregates to single particles.

Prior to grain-size analysis, removal of organic matter and calcium carbonate was performed (see details in Konert and Vandenberghe,

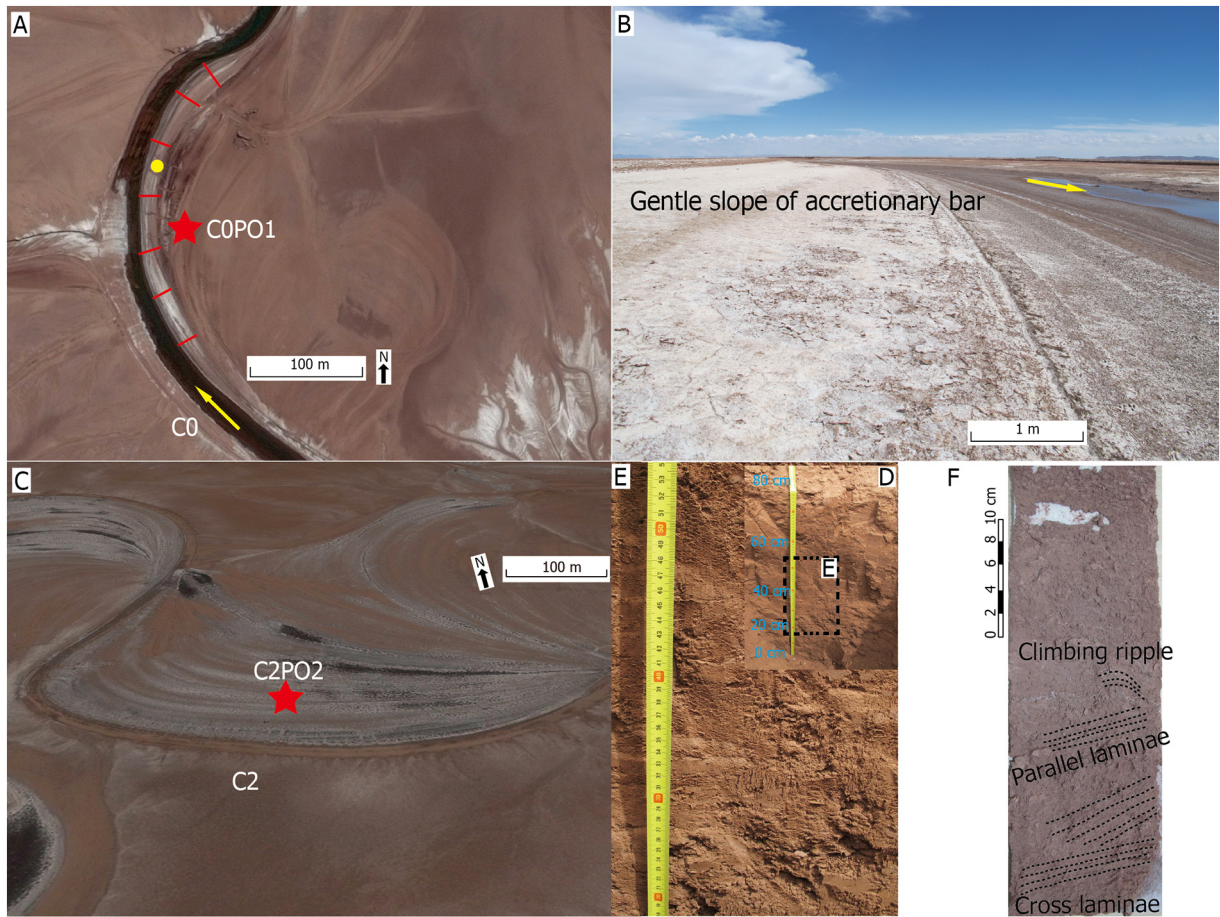


**Fig. 2.** Examples of present accretionary bar (C0PO1) and borehole locations in the meander bend (C2PO2). A) The red lines indicate the width of the present accretionary bar and the yellow dot shows the position where the photograph B was taken. B) The field photograph indicates the gentle slope of the present accretionary bar. D) and E) Details of borehole images of C2PO2. F) and G) Lacquer peel from the upper 40 cm of borehole C2PO2 and its interpretation. Sedimentary structures are visualised on lacquer peels. Asterisks in A and C show borehole locations in the present and abandoned meander bends (A: C0PO1 and C: C2PO2). (For interpretation of the references to colour in this figure legend, the reader is referred to the web version of this article.)

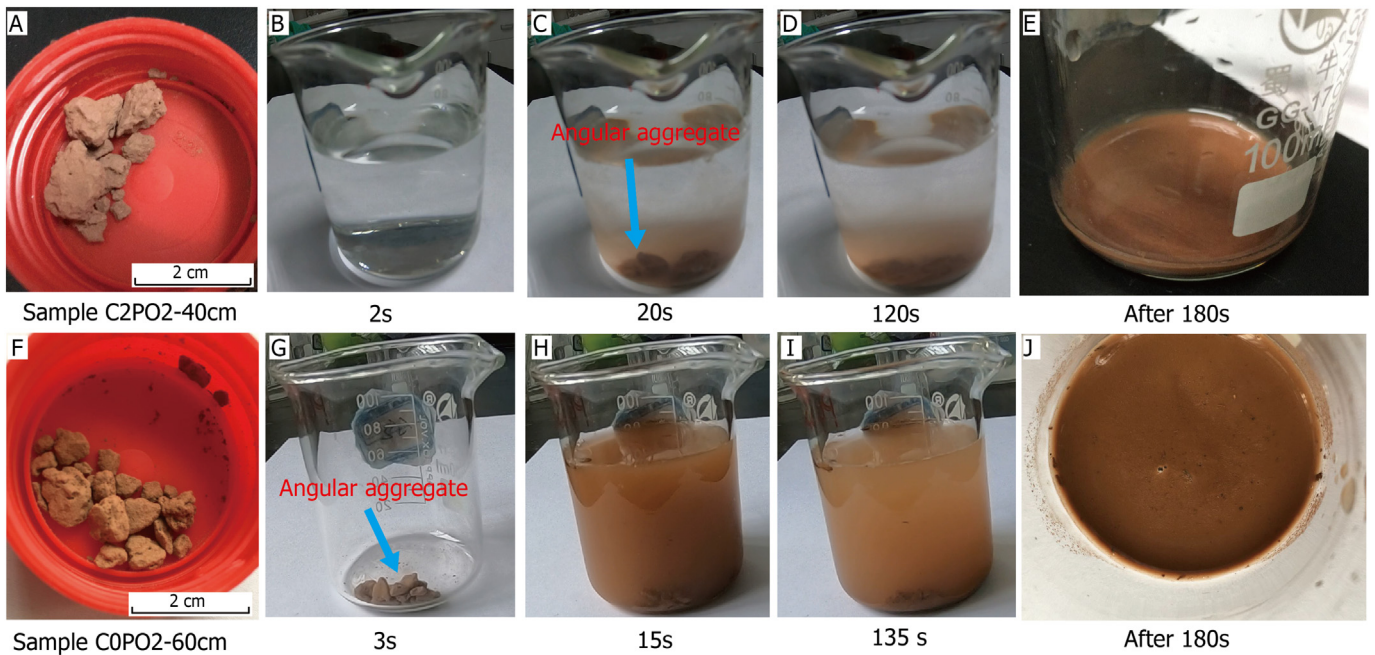


**Fig. 3.** Dispersal processes of two samples from borehole C2PO2 at 40 cm depth (A-E) and from borehole C0PO2 at 60 cm depth (F-J). A-E) Depiction of the experiment; adding aggregates in the standing deionised water. F-J) Deionised water poured in the beaker with mud aggregates. Diameter of beakers is 5.5 cm.

1997). Samples were then measured by a laser-diffraction particle sizer with a range from 0.1 to 2000  $\mu\text{m}$ . To quantify the influence of sample selection on the grain-size distribution results, additional duplicate measurements (three samples with random selection) were performed (Fig. 4).

Grain-size distributions are widely used for interpreting sedimentary processes and environmental dynamics (Prins and Weltje, 1999; Prins et al., 2000; Vandenberghe, 2013). End-member modelling analysis (EMMA) based on the principles of numerical inversion has been successfully used to decompose grain-size populations as a linear combination of end-member (EM) loadings and scores (Weltje, 1997; Prins et al., 2000). Loadings are genetically interpretable grain-size distributions, whereas scores are relative contributions of different EMs to each sample (Weltje, 1997). An open-source modelling package, EMMAgeo, using the software R was employed to extract different end members (see detailed methodology in Dietze et al., 2012, 2014; Dietze and Dietze, 2013; Dietze et al., 2016). The modelling results

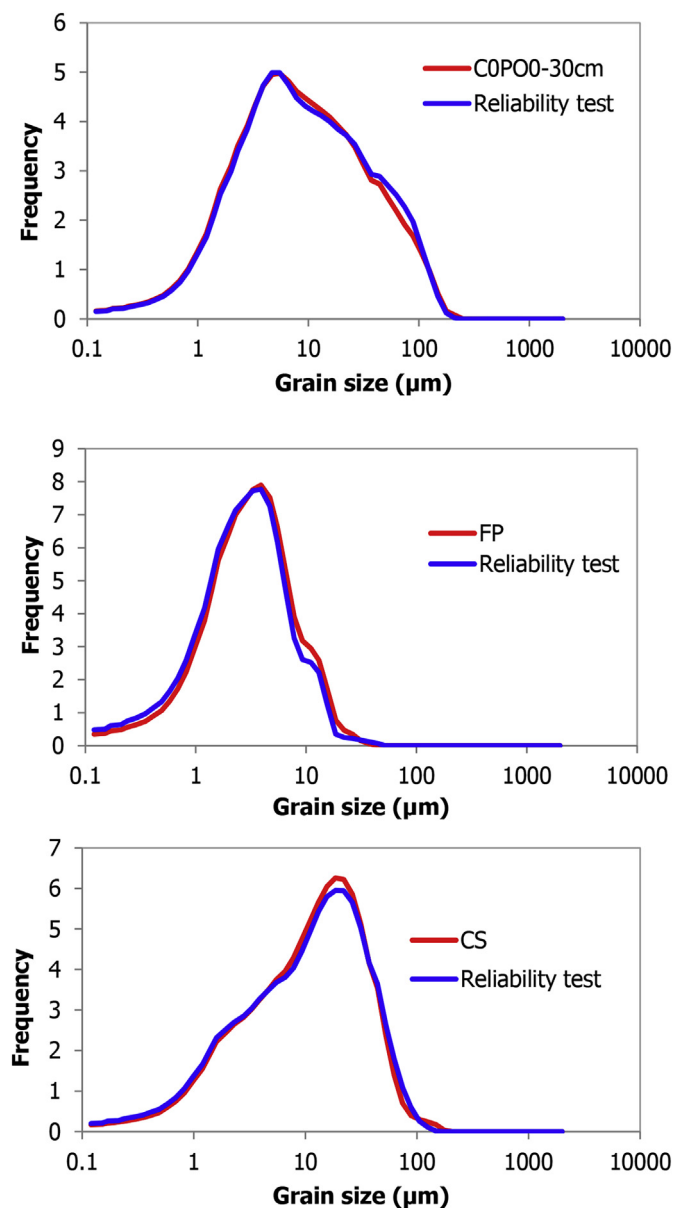


Fig. 4. Duplo-measurements of grain-size distribution of three samples from different sedimentary elements. COPO1–30 cm is borehole COPO1 from the point bar deposits. FP indicates sample from floodplain, whereas CS shows samples from crevasse splay.

depend on the number of EMs and the range limits for data scaling with a weight transformation (Dietze et al., 2012; Dietze et al., 2016). The weight transformation includes a quantile range (“percentile”), which may vary from zero to the maximum quantile (the highest possible quantile) aimed at numerically stable weight transformations (Dietze et al., 2016). The grain-size data of the 219 sediment samples from the study area were used as input to define an optimal number of end members and the quantile range through the EMMAgeo package. The optimal number of EM was determined by mean total, row-wise (sample-wise) and column-wise (class-wise)  $R^2$  between original and modelled data (Dietze et al., 2016). Secondary modes could occur for EMs as a consequence of either the measurement procedures employed or of sedimentary processes (Dietze et al., 2014). Such secondary modes cannot be avoided for end-member modelling because of the nature of the technique, including measurement procedures and sedimentary processes (Prins and Weltje, 1999).

### 3.2.2. Loss on ignition (LOI) and mineralogy

To quantify sediment compositions such as organic matter and clay minerals, which play an important role in mud aggregation and dispersion, loss on ignition (LOI) and X-ray diffraction (XRD) were used in the study. The content of organic matter and carbonates was measured by Loss on ignition (LOI) (Heiri et al., 2001). Using a Leco TGA 601 apparatus, the organic matter content was determined by oxidising the samples at 500–550  $^{\circ}\text{C}$  to obtain the organic matter content, and then by heating the sample to 900–1000  $^{\circ}\text{C}$  to determine the carbonate content. Attempts to conduct palynological analysis proved futile due to a lack of pollen in the samples.

X-ray diffraction (XRD) was performed to quantitatively determine the clay mineralogy, in particular the content of smectite that may play an important role in grain aggregation (Maroulis and Nanson, 1996; Wright and Marriott, 2007). The sediment samples were air-dried and ground to powder size in a small agate mortar using an agate pestle. Samples were sieved to obtain the fraction of 0.063–0.125 mm and randomly oriented powders were prepared for XRD analysis, which was carried out on an X’ Pert Pro diffractometer with Ni-filtered  $\text{Cu K}\alpha$  radiation (40 kV, 40 mA, wavelength: 0.15416 nm). Heating and glycolation were used for the fraction of <0.002 mm to further distinguish and quantify the content of clay minerals such as smectite and illite (for details of heating and glycolation see Wang et al., 2017). The scanning range used was  $3\text{--}65^{\circ} 2\theta$  and the scan rate was  $0.42^{\circ} 2\theta$  per second with a step size of 0.017. The program SYB-ILLA (©Chevron) was used to identify the mineralogy of the tested samples.

### 3.2.3. Characteristics of decadal deposits in the distal system

Bi-temporal high-resolution satellite imagery (2005 and 2016) from Google Earth Pro™ were used to show areas where only salt deposits were observed before 2005, indicative of limited mud deposits, but which on the image of 2016 were covered by recent mud deposits due to river avulsion and progradation that post-dated the acquisition of the 2005 imagery. Daily precipitation data were collected in the study area for the period 2004 through 2017 from the Bolivian Servicio Nacional de Meteorología e Hidrología. The aim of the grain-size analysis of the deposits at the trench COD was to investigate the nature of sedimentation and its relation to changes in magnitude of precipitation in the Río Colorado terminus.

## 4. Results

### 4.1. Channel characteristics

The Río Colorado river terminus is characterised by a superposition of different events of river channel development, although generally only a single channel is thought to have been active for a given period (Donselaar et al., 2013). Ridge-and-swale topographies of point bars

are difficult to recognise in the field but are detectable by the differential salt cover (Donselaar et al., 2013), which can be seen clearly on high-resolution satellite imagery (Fig. 2C). Field observation revealed these bars to be composed of point-bar accretion layers (Fig. 2B). The inner bank slope of the present-day channel dips, on average, at 4.1° (range 3 to 7°) (Fig. 2A, B). Desiccation cracks and salt efflorescence are well

developed on the reddish-brownish oxidised surfaces (Li and Bristow, 2015). Trench data indicate that the point-bar deposits are compacted and cemented, and oblique and cross-lamination structures have exceptionally been observed on laquer peels (Figs. 2F, 5). Erosional surfaces were not identified in the trenches because the sediment is mud and no clear changes could be observed by eye either in colour or grain size.

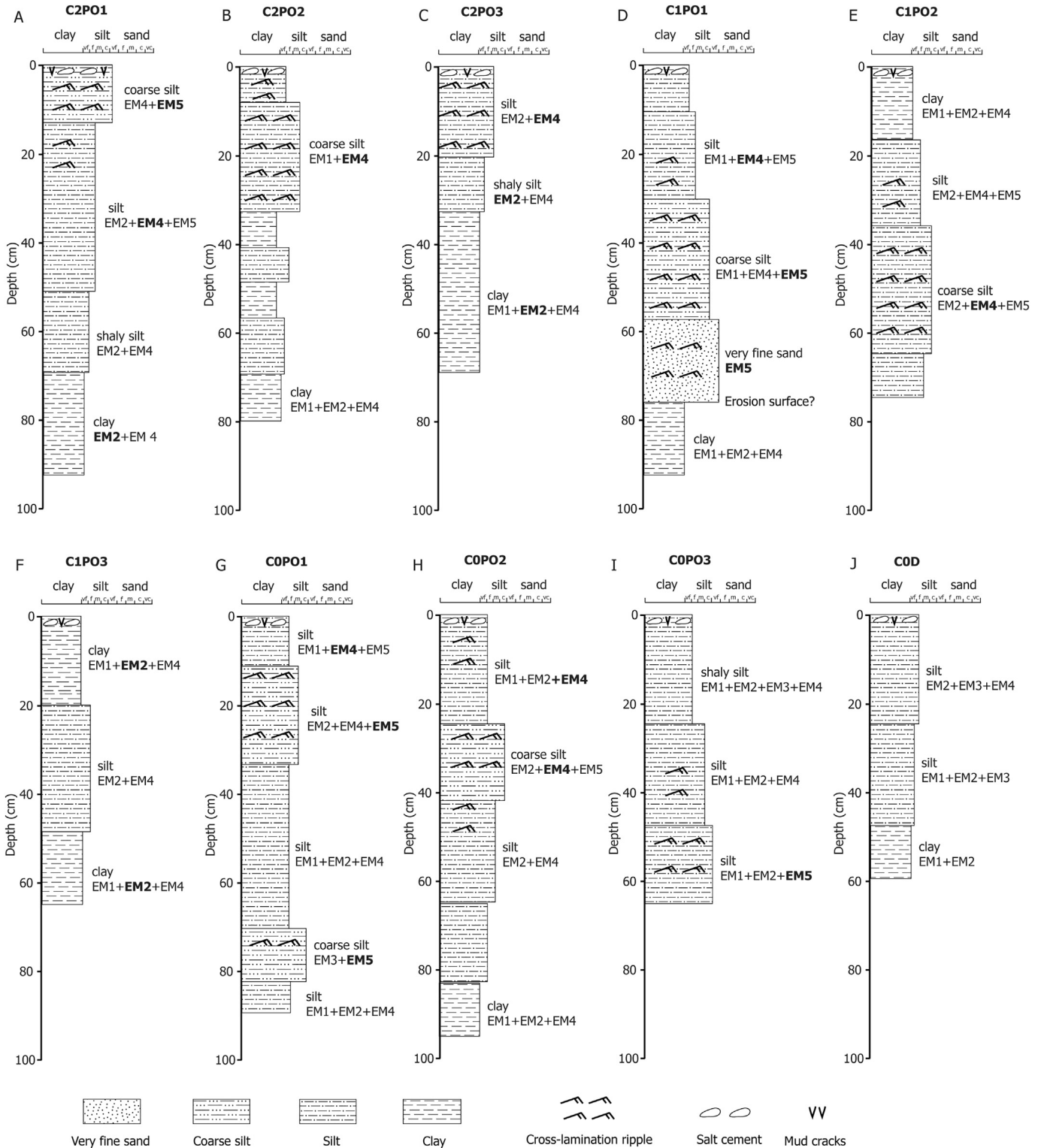


Fig. 5. Sedimentary logs of trenches along the channels in the study: A–C: C2; D–F: C1; G–J: C0. Endmembers (EMs) derived from modelling are labelled on the corresponding parts of logs with EMs reported in bold indicative of dominant components.

**Table 1**  
Statistics of duplo-measurements of GSD.

Sample	Median ( $\mu\text{m}$ )	Mean ( $\mu\text{m}$ )	St. Dev.	Skewness	Kurtosis
COPO0–30 cm	7.28	7.05	1.98	0.13	2.72
COPO0–30 cm-RM	7.58 (4%)	6.98	1.99	0.15	2.67
FP	2.83	8.57	1.4	0.49	3.46
FP-RM	2.55 (9%)	8.74	1.43	0.49	3.4
CS	10.53	6.89	1.83	0.66	3.14
CS-RM	10.37 (2%)	6.94	1.9	0.66	3.01

FP: floodplain; CS: crevasse splay; RM: duplicate measurement. Percentages in brackets are difference in median value between first measurements and duplicate measurements.

#### 4.2. Grain-size analysis

The experiments with two scenarios of hydraulic conditions show that nine samples of aggregates were capable of dispersing into single particles in <2 min in either standing or flowing water (Fig. 3). The angular aggregates were quickly saturated by water and dispersed into single particles. Given the results of these experiments, we believe that most particles were not transported as aggregates, and that therefore the measured grain-size distributions are representative of the suspended-load composition.

The grain-size distributions are characterised by only very small differences in the duplicate tests (Fig. 4, Table 1) showing only minor differences in statistic bulk parameters, such as  $D_{50}$  and standard deviation. Given the favourable duplicate test results, we are confident that

the grain-size distributions determined using the laser-diffraction particle sizer are appropriate to characterise these fine-grained sediments. The raw grain-size distribution of 219 sediment samples shows that the sediments are dominantly unimodal in the river terminus. These samples consist primarily of fine-grained sediments with a maximum  $D_{50}$  of 52  $\mu\text{m}$ , a minimum  $D_{50}$  of 2.8  $\mu\text{m}$  and a mean  $D_{50}$  of 8.2  $\mu\text{m}$  (Fig. 6). In the proximal area of the terminus (boreholes C2PO1, C1PO1, COPO1), the grain-size distributions are mainly bi- to multi-modal, whereas the distal area of the terminus is dominated by unimodal distributions (C2PO3, C1PO3, COPO3). The proximal point-bar deposits of channel C1 with mean  $D_{50}$  of 24  $\mu\text{m}$  (9 samples) – and the maximum  $D_{50}$  up to 52  $\mu\text{m}$  and the minimum  $D_{50}$  up to 6  $\mu\text{m}$  – are coarser than the proximal deposits of channels C0 (17 samples) and C2 (19 samples), where  $D_{50}$  values are mostly <20  $\mu\text{m}$ , the mean  $D_{50}$  being 11  $\mu\text{m}$  for C2PO1, and 12  $\mu\text{m}$  for COPO1 (Fig. 6).

Two contrasting vertical successions of point-bar deposits have been detected: coarsening-upward and fining-upward deposits. For three point bars of channel C2, a clear coarsening-up succession has been identified by  $D_{50}$ , especially for C2PO1 in the proximal part of the river terminus (Fig. 7). This borehole shows a strong coarsening-upward trend in 10-cm intervals for  $D_{50}$ , with a small  $D_{50}$  of 6  $\mu\text{m}$  at the bottom and a largest  $D_{50}$  of 23  $\mu\text{m}$  at the surface. By contrast, two of the three point bars examined in channel C1 (C1PO1 and C1PO2) exhibit a prominent fining-upward trend. For channel C1, only C1PO3 exhibits a coarsening-upward trend. For instance, in C1PO1, the  $D_{50}$  decreases from 52  $\mu\text{m}$  at a depth of 0.7 m to 7  $\mu\text{m}$  at the surface of the point bar; this succession overlies much finer sediment at 0.8 m depth. For the

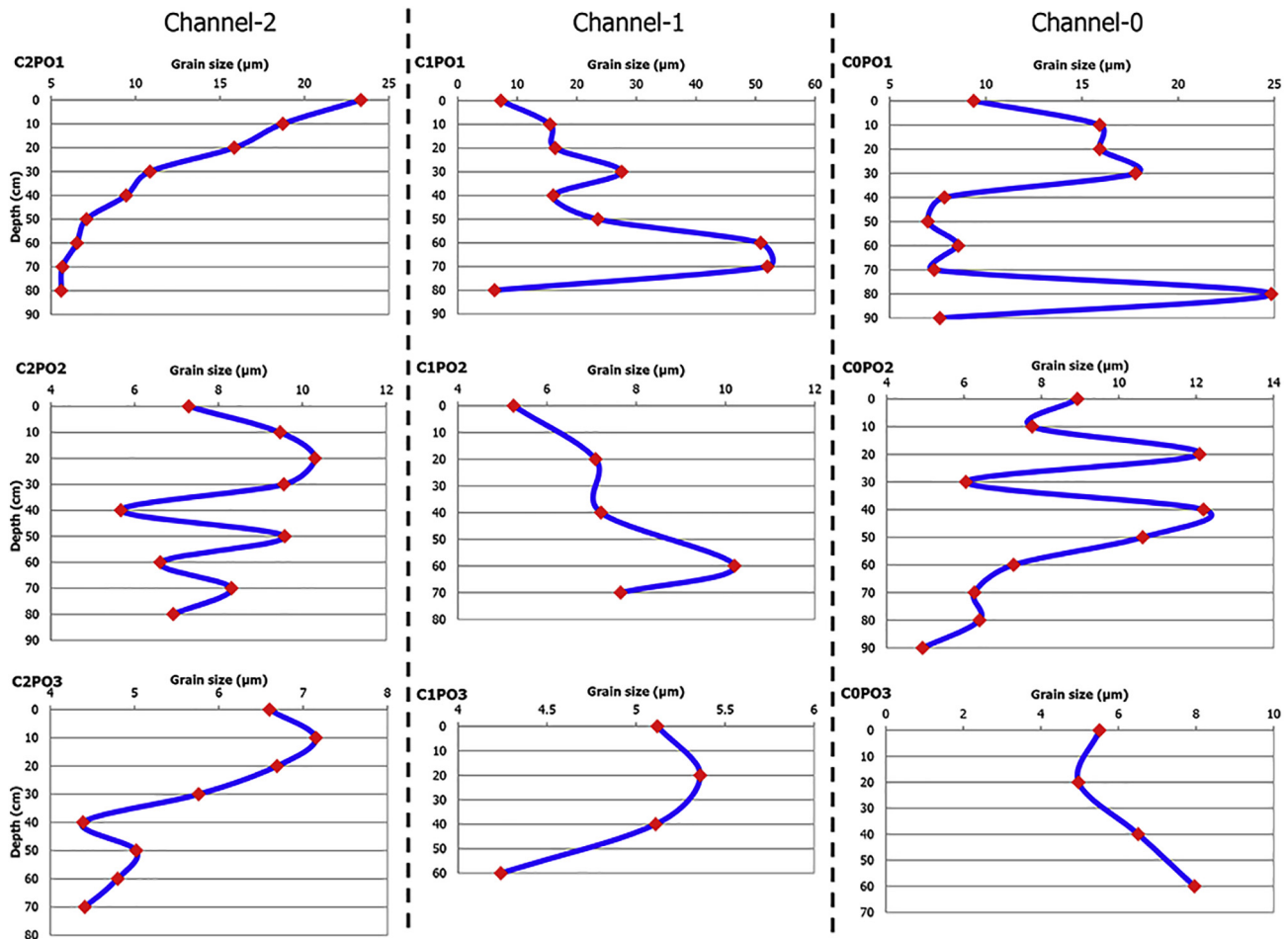


**Fig. 6.** Vertical changes in median value ( $D_{50}$ ) of point-bar deposits in the terminus system. Channel-2 (C2) was active in the period 1.1–0.9 ka, channel-1 (C1) was active in the period 0.7–0.5 ka whereas channel-0 (C0) is presently active (0.4 ka–present). C2PO1, C2PO3 and COPO2 are characterised by a coarsening-upward sequence, whereas C1PO1 and C1PO2 are characterised by a fining-upward sequence.

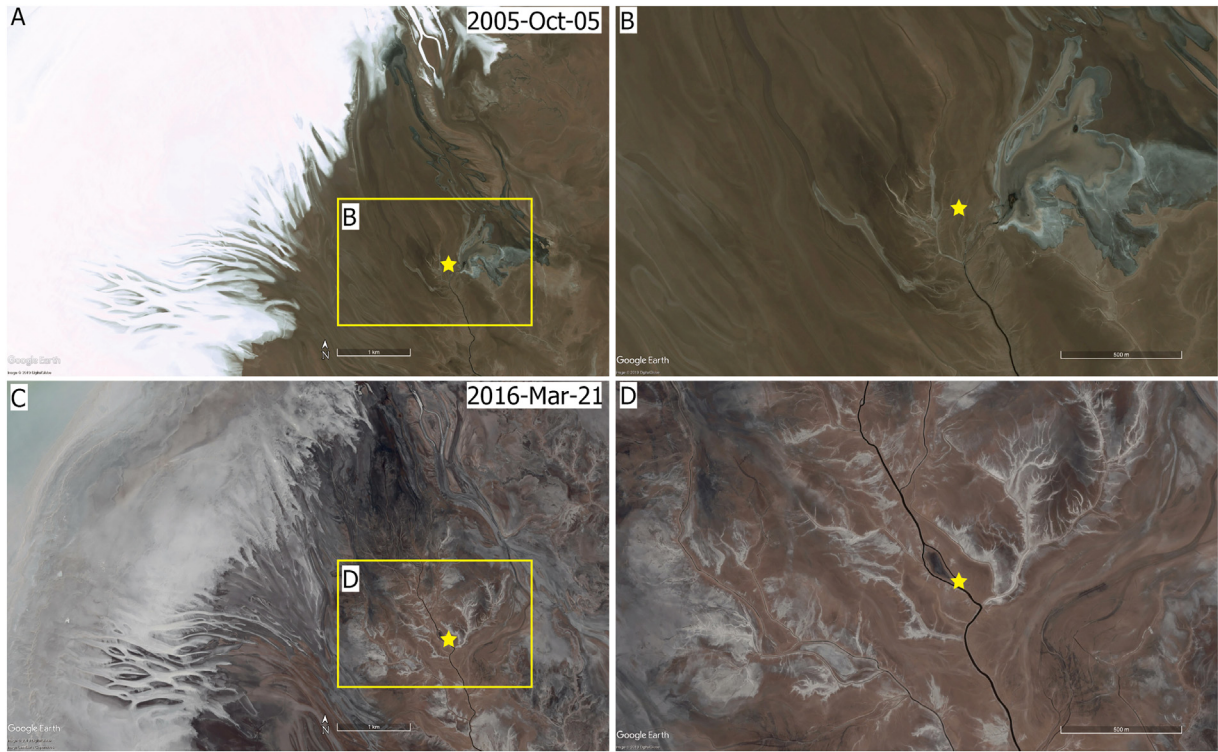


**Fig. 7.** Decadal bi-temporal satellite imagery (2005 and 2016) indicating aggradational processes in the distal part of the Río Colorado terminus system. Asterisks are indicative of the same location.

active channel C0, only COPO2 exhibits a clear coarsening-upward trend with a small  $D_{50}$  of  $5\ \mu\text{m}$  at the bottom and a large  $D_{50}$  of  $12\ \mu\text{m}$  in the upper part of the trench. COPO1 shows a fluctuating variation in  $D_{50}$  on the profile.

Prominent channel morphology and deposits at locality COD in the distal region for a decadal observation period provided an opportunity to examine the response of sedimentation patterns in the Río Colorado terminus to changes in magnitude of precipitation. Bi-temporal satellite imagery (2005 and 2016) from Google Earth Pro™ indicates that the currently active main channel (C0) in the distal part of the river

terminus extended over the previous site of fluvial termination (Fig. 7A, B) and prograded toward the salt lake (Fig. 7C, D).

Daily precipitation data record an overall increasing trend in the maximum daily precipitation between 2005 and 2016 (Fig. 8A). Additionally, the upper part of the sediment profile in the distal part of the river terminus is characterised by a pronounced coarsening-upward succession (Figs. 5J, 8B). Such consistency between the upward increase in the sediment calibre of the distal deposits, and the increase in the magnitude of maximum daily rainfall, suggests a positive causative relationship between flow regime and deposition. For this short period

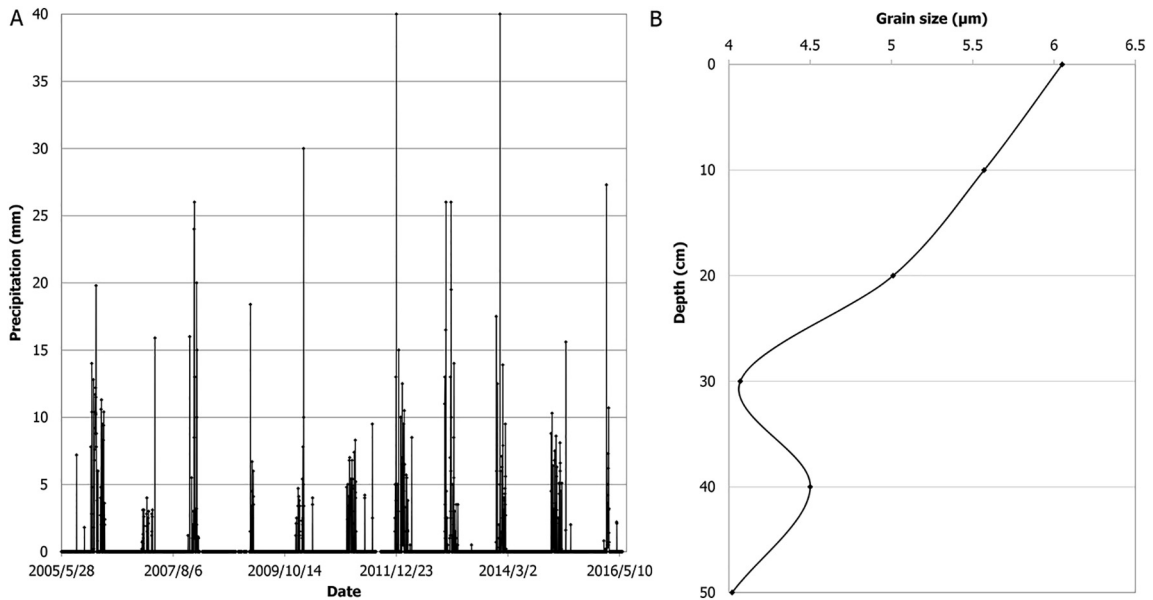


**Fig. 8.** A) Daily precipitation between 2005 and 2016. B)  $D_{50}$  of sediments at the distal part of the river terminus. See the location in Fig. 6.

there has been no discernible tectonic activity, longitudinal gradient or vegetation cover, and the catchment overall remains unchanged.

#### 4.3. Post-processing of grain-size data (EMMA)

The EMMA analysis was applied to extract subpopulations of grain-size distributions of the samples (Fig. 9). The modelling results show that the explained variance ( $R^2$ ) is at its maximum value and stable between four and five EMs (Fig. 9A). However, the mean row-wise and column-wise  $R^2$  values (0.83) for five EMs are higher than that for four EMs (0.81) indicating that the best performance for the EM number is 5 (Fig. 9B). More EMs could explain a larger proportion of measured distributions; however, more than five EMs do not mean a significant unmixing improvement in this study, and in some cases such results do not have a geological meaning (Weltje, 1997; Dietze et al., 2012). Therefore, for the samples from the study area, five EMs have been selected. These five EMs are characterised by prominent individual modes at 2  $\mu\text{m}$  (EM1), 4.6  $\mu\text{m}$  (EM2), 11  $\mu\text{m}$  (EM3), 22  $\mu\text{m}$  (EM4) and 88  $\mu\text{m}$  (EM5), respectively (Fig. 9C).

EMMA reveals that the three channels are characterised by marked differences in their proportions of the five EMs. For instance, the proportions of EM5 show a prominent downstream reduction from the

proximal to distal parts of the three channels (Fig. 10). In addition, for single boreholes, EMMA also quantifies vertical variations in the proportion of the different EMs, revealing two distinct vertical successions of point-bar deposits: coarsening-upward and fining-upward. The coarsening-upward succession is characterised by a high proportion of fine EMs in the bottom part and an increasingly high proportion of coarser EMs toward the top. For instance, C2PO1 is dominated by three EMs: EM2, EM4 and EM5. EM5 increases from <4% at the bottom to almost 80% at the top, but EM2 shows a decreasing trend from up to 60% at the bottom to none on the top, though EM4 appears to be quite constant (see C2PO1 in Channel-2, Fig. 10). Likewise, other boreholes for C2 (C2PO2 and C2PO3) and C0 (C0PO2) show similar vertical patterns (see Channel-2 and Channel-0, Fig. 10). For fining-upward deposits, coarse EMs generally dominate at the bottom but decrease to the surface, whereas fine EMs have an inverse trend within one borehole. For instance, EM5 dominates at the bottom of borehole C0PO3 and fine EMs increase upwards.

#### 4.4. LOI results and mineralogy

The LOI results show that the contents of organic matter and carbonate are generally low (Fig. 11). In C2PO1 they are lower than 1% and 4%,

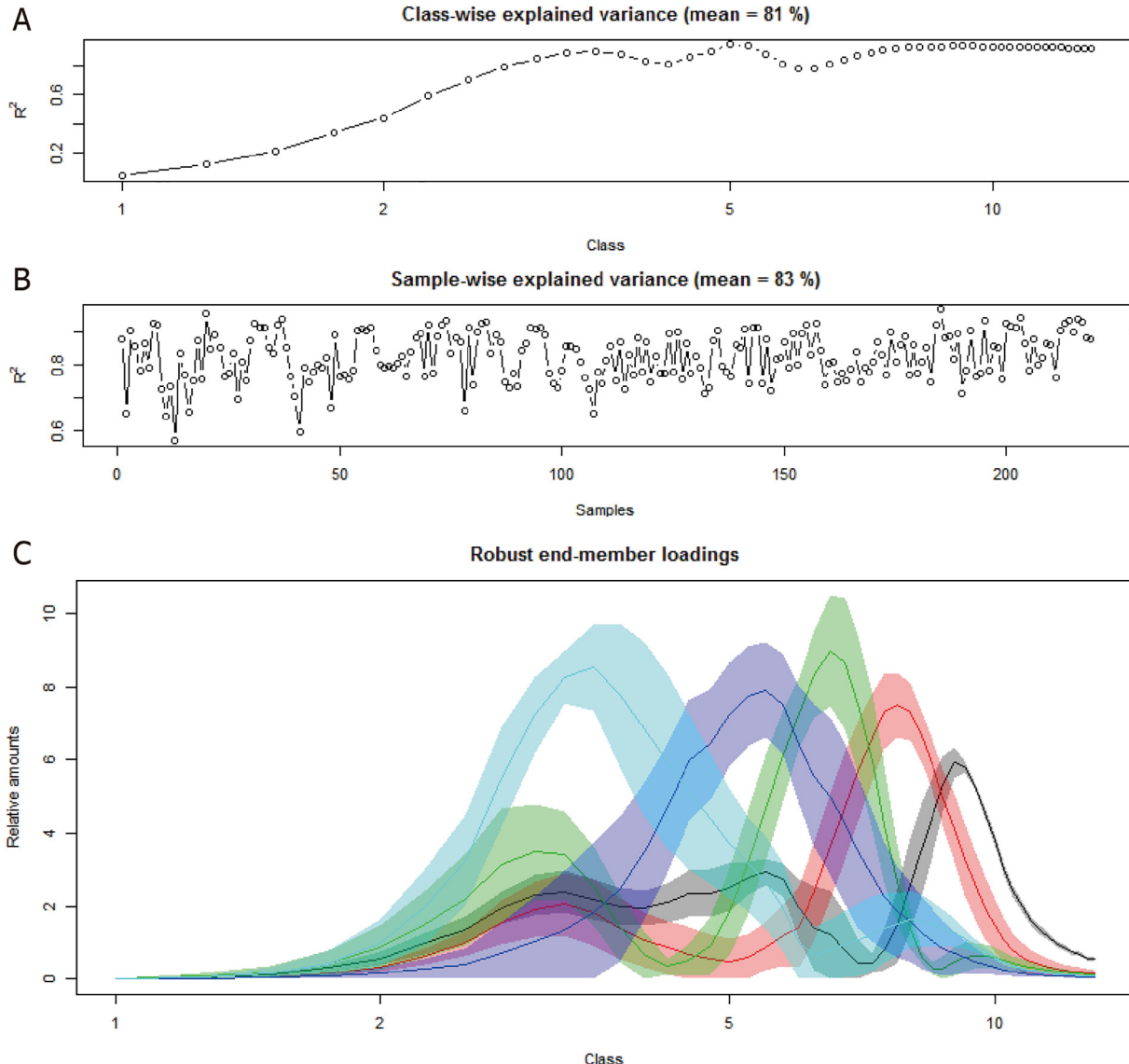
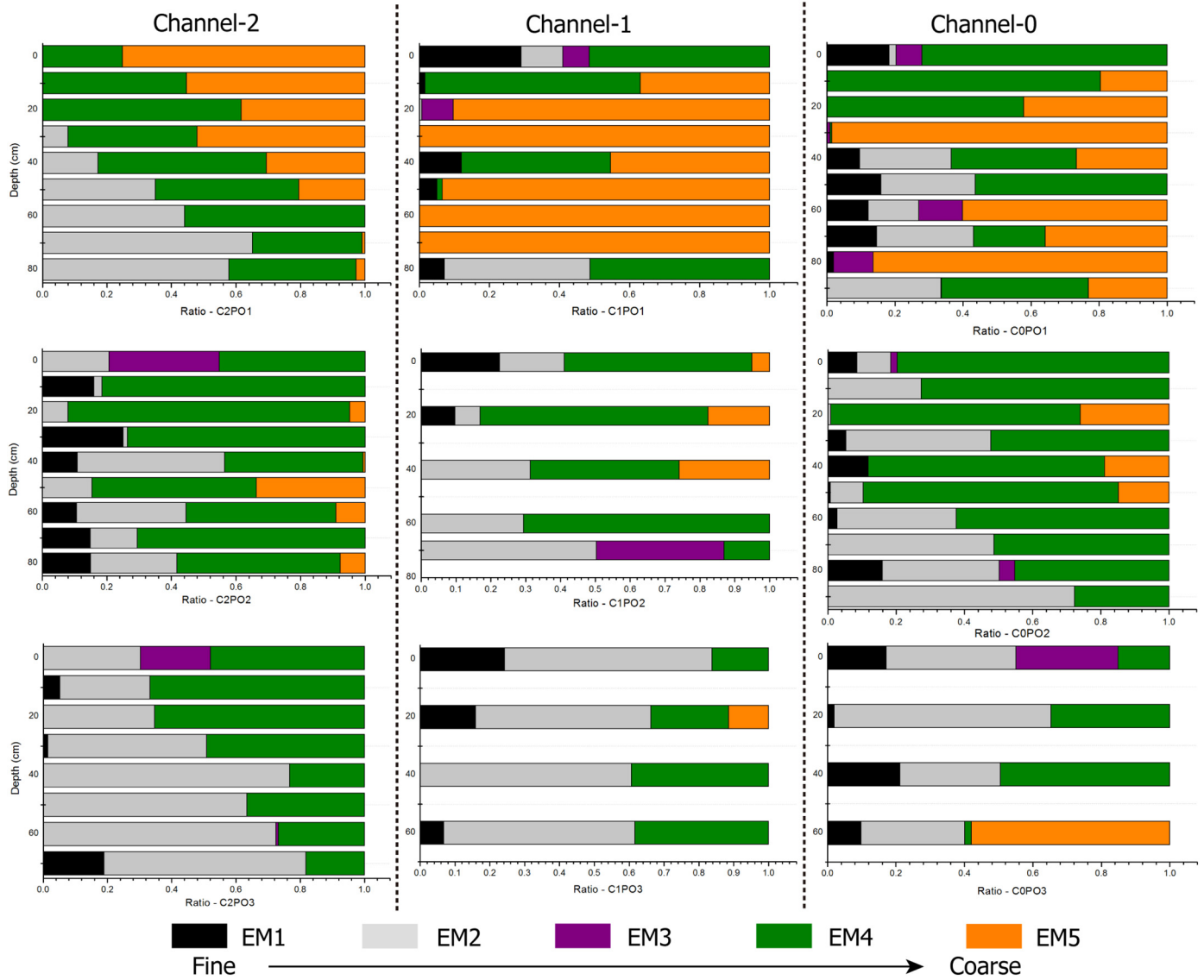


Fig. 9. End-member modelling results. A) and B) Class-wise and sample-wise explained variance, respectively. C) End-member loadings.



**Fig. 10.** Evolution of EM percentages as a function of depth for the various sites (location in Fig. 1D). C2PO1, C2PO3 and C0PO1 show an upward increase in coarse EMs, whereas C1PO1, C1PO2 and C1PO3 indicate an upward increase in fine EMs. The arrow indicates changes from fine EM1 to coarse EM5.

respectively, except at the surface where a slight increase is seen. In contrast, the LOI results for borehole C1PO1 and C0PO1 were up to 2.7% in organic matter and 7% in carbonate with strong fluctuations, but overall, they were significantly higher than in borehole C2PO1 (Fig. 11).

XRD analysis of the 0.063–0.125 mm fraction of 15 samples randomly selected shows that illite, quartz and albite account for 80% and other minerals, such as halite, pyrite, calcite and clinocllore for <20%. Further heating and glycolation analysis of the <0.002 mm fraction of nine samples show that the clay minerals include smectite, interlay smectite-illite, illite, kaolinite and chlorite (Fig. 12). On average, the interlay smectite-illite is about 52%, illite is about 23% and smectite accounts for about 19%. Kaolinite and chlorite are <8% and 3%, respectively (Table 2).

**5. Interpretation of endmember (EM) transport modes**

Characteristics of EMs provide a unique opportunity to interpret the transport modes of individual EMs. The coarsest EM5 is apparently a channel sediment as wind-driven saltation transport in the Río Colorado terminus is limited due to salt cementation at the surface (Donselaar et al., 2013). However, sediments deposited from suspended-load

fallout from aeolian transport seem to be represented as the widely occurring EM4, with a grain-size distribution (22 μm) resembling very well that of a loess transported in suspension at low elevation over relatively short distances (Vandenberghe, 2013). The quite rarely occurring EM3 has a smaller grain-size distribution (11 μm), which is also typical for suspended wind transport, but rather at higher elevation and over longer distances (Vandenberghe, 2013). An aeolian origin (loess) for both EM3 and EM4 does not preclude the opportunity for later (secondary) fluvial transport. It has indeed been shown that the average, original aeolian grain-size distribution is not really changed by the later fluvial reworking (Vandenberghe et al., 2010, 2012, 2018). Thus, EM3 and EM4 may be ultimately transported in a suspended mode by the river as fluvially reworked aeolian deposits. Field observations reveal an increased incidence of cross lamination in sediments with high proportions of EM4 and EM5 (Fig. 5).

EM2 is, in fact, a clay in the traditional sense (as measured by laser diffraction: Konert and Vandenberghe, 1997). Most logically it could only be deposited in standing water. Its occurrence implies the development of standing pools of water on the floodplain in the aftermath of flooding events. Originally it may have been sorted from fine-grained (reworked) loess EM3–4. As the final deposition was in standing

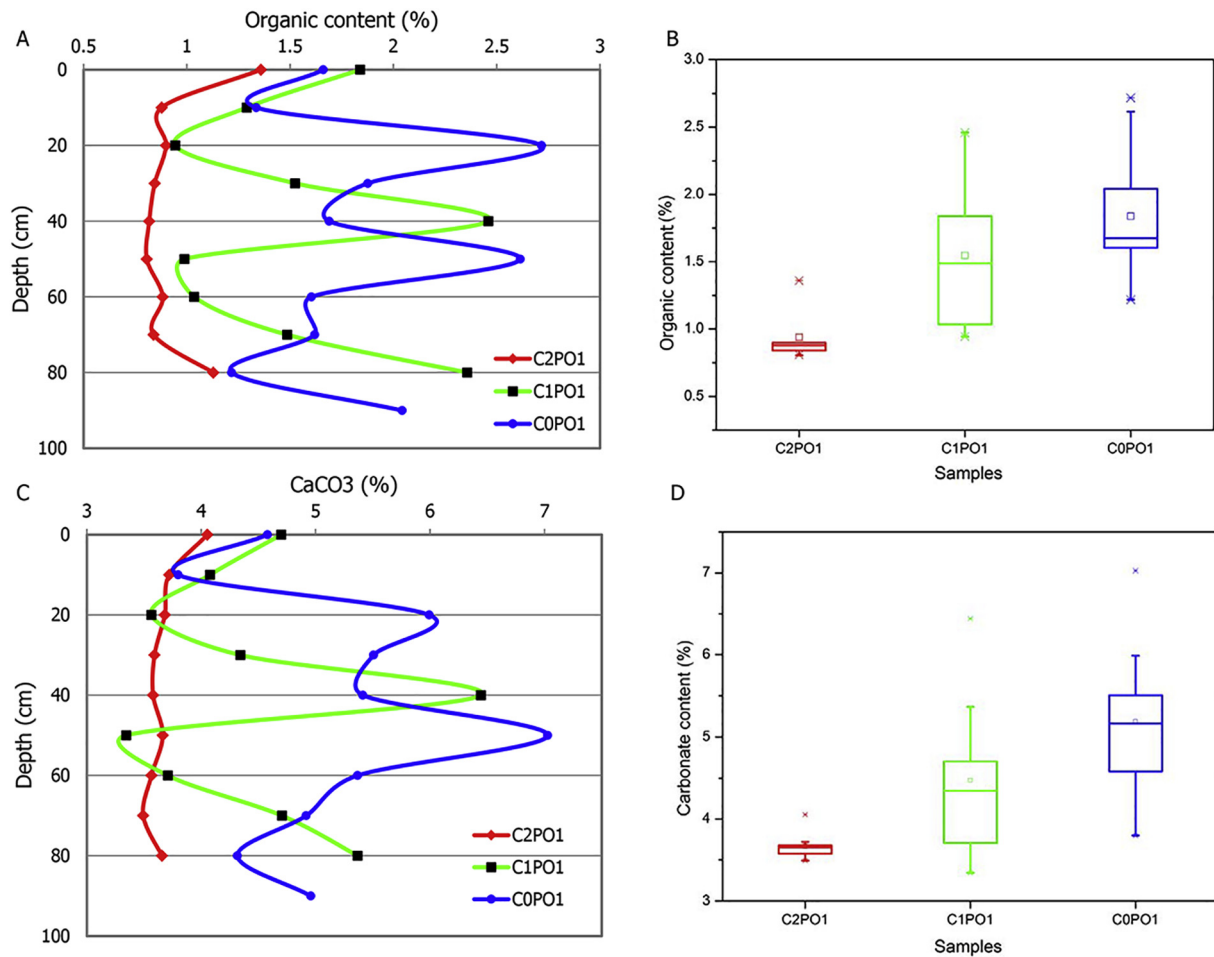


**Fig. 11.** A) and B) Results and statistics of organic content through loss-on-ignition at 0–550 °C; C) and D) Results and statistics of carbonate content through loss-on-ignition at 550–950 °C for point-bar deposits in the proximal area of the terminus.

water on the floodplain, it might be a lacustro-aeolian deposit (Vandenberghe et al., 2018). Satellite imagery indicates that the episodic development of an extensive body of standing water across the floodplain after peak flood (Li et al., 2018), despite the system being entirely dry during field campaigns. Additionally, prior field observations reveal prominent desiccation cracks (Fig. 5) (Li and Bristow, 2015).

Finally, EM1 is fine clay to which a pedogenic origin is attributed (e.g., Sun et al., 2006; Sun et al., 2011; Zeeden et al., 2016). It also occurs in low amounts throughout the sections. Whether it is formed primarily (in situ) or has been reworked by the river and deposited in pools as EM2 cannot be ascertained from the grain-size distribution.

## 6. Discussion

### 6.1. Sediment transport in very fine-grained meandering river terminus systems

The deposits of the Río Colorado meandering terminus system are predominantly fine-grained with  $D_{50}$  of  $<10 \mu\text{m}$ , which is finer than other documented fine-grained meandering river systems (e.g., sandy silt-dominated Río Bermejo with a  $D_{50}$  of up to  $182 \mu\text{m}$ ; Sambrook Smith et al., 2016). Despite progradation of the fluvial system in a lake-level lowstand, this outcrop of recent point-bar deposits provides an excellent opportunity to examine laterally accreting features that are easily identified by both field observation and high-resolution ( $<0.65 \text{ m}$ ) satellite imagery (e.g., Fig. 2A, B, C) in the Río Colorado terminus system. The Río Colorado meandering terminus system is notably

different from other documented modern fine-grained river systems in terms of vegetation cover and mineralogical composition (Maroulis and Nanson, 1996; Wakelin-King and Webb, 2007; Sambrook Smith et al., 2016). First, it is non-vegetated due to the hyper-arid climate and salt-rich conditions in the study area (Li and Bristow, 2015). Meteorological data have revealed that the annual precipitation is 184 mm (Li, 2014); the maximum temperature is 21.1 °C in November and the minimum temperature  $-9.3 \text{ °C}$  in July (Lamparelli et al., 2003). This absence of vegetation is also consistent with the low organic matter content (Fig. 8), which could reduce the cohesion of sediment and hinder aggregation. However, other fine-grained meandering systems are characterised by dense or sporadic vegetation cover (Jackson, 1981; Page et al., 2003; Wakelin-King and Webb, 2007; Sambrook Smith et al., 2016; Slowik et al., 2020). Field campaigns also revealed that lateral accretion processes dominate and obliquely accreted banks have been rarely seen in the Río Colorado meandering terminus system, though the  $D_{50}$  of sediment in this system is  $8.2 \mu\text{m}$  in a silt-clay class. In contrast, some rivers with more silt to clay sediment might tend to have obliquely accreted banks (e.g., Klip River in South Africa, Marren et al., 2006; Río Bermejo in Argentina, Sambrook Smith et al., 2016; the Kapos and Koppány valleys in Hungary, Slowik et al., 2020).

Second, variations in mineral compositions exist between the Río Colorado terminus system and other fine-grained systems (e.g., Maroulis and Nanson, 1996; Gibling et al., 1998; Wakelin-King and Webb, 2007). Multi-treatment XRD analysis revealed that smectite is about 19% in the point-bar deposits in the Río Colorado meandering terminus system. However, laboratory analysis indicated that these

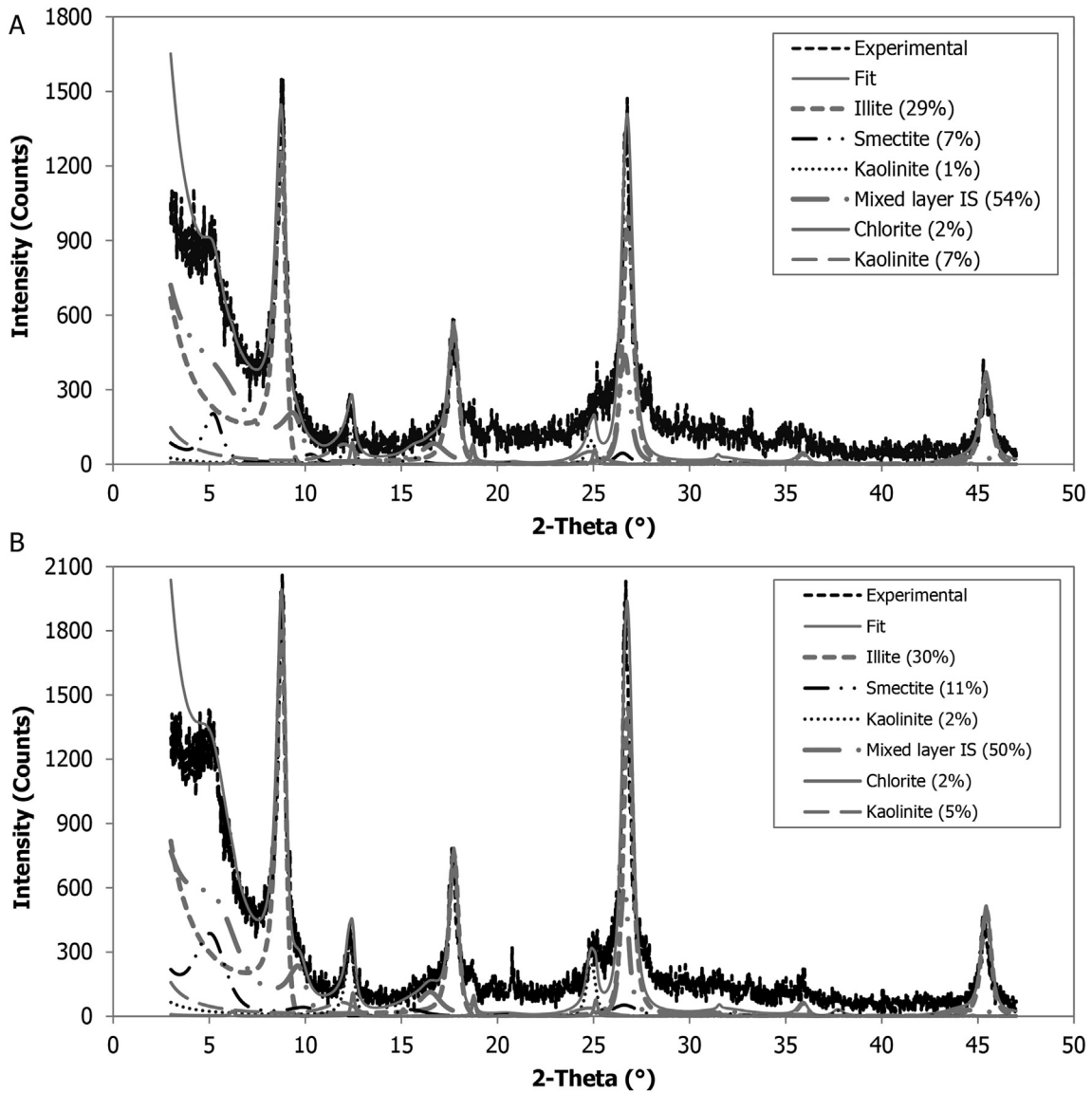


**Fig. 12.** Examples of results of X-Ray diffraction (XRD) profiles using the program SYB-ILLA (©Chevron). A) Sample from 0.3 m depth in borehole C2P01; B) Sample from 0.4 m depth in borehole C1P01.

aggregates were dispersed in standing deionised water for <2 min and this process tended to be faster if any continuous stirring such as flowing water was implemented so that individual minerals became visible (Fig. 3). The experimental analysis on the dispersal of aggregates suggests that the majority of aggregates are unlikely to survive transport during flooding, though more quantitative methods are required to investigate the roles (or behaviour) of clay minerals in aggregate dispersal. Notably, single gravelly aggregates were not observed in the Río Colorado terminus system whereas they are observed in central Australia where smectite dominates the clay mineralogy (Maroulis

and Nanson, 1996). In central Australia, swelling clays including smectite trigger aggregation coupled with wet-dry cycles and pedogenesis (Rust and Nanson, 1989; Maroulis and Nanson, 1996; Gibling et al., 1998; Wakelin-King and Webb, 2007). Studies on ancient outcrops (e.g., the Lower Permian Clear Fork Formation) reveal that even in the absence of the strong swelling component smectite but the presence of minor amounts of the swelling illite component could lead to aggregation. Mud aggregates were well preserved in point-bar deposits due to rapid incorporation into a developing (i.e., actively migrating) point bar and limited compaction effects (Simon and Gibling, 2017a). These

**Table 2**  
Results of XRD analysis for <0.002 mm fraction of the samples.

Clay minerals	COP01-40 cm	COP02-40 cm	C1P01-40 cm	C1P02-0 cm	C2P01-10 cm	C2P01-30 cm	C2P01-60 cm	C2P02-40 cm	C2P03-0 cm
Illite	0.22	0.2	0.3	0.4	0.11	0.29	0.23	0.25	0.08
Smectite	0.05	0.27	0.11	0.06	0.44	0.07	0.2	0.09	0.44
Kaolinite	0.05	0.03	0.07	0.03	0.03	0.08	0.03	0.07	0.02
Mixed layer Illite Smectite	0.65	0.5	0.5	0.48	0.41	0.54	0.53	0.58	0.46
Chlorite	0.03	0.01	0.02	0.03	0.01	0.02	0.01	0.01	0.01

prominent distinctions between the modern outcrop of the Río Colorado terminus system and the ancient outcrop of the Lower Permian Clear Fork Formation require further research to quantify the impacts of various clay minerals and their combination on aggregation. Additionally, dispersal ability of mud aggregate, which plays an important role in sediment transport in the fine-grained river terminus, should also be quantified in future research.

### 6.2. A conceptual model for the upward-coarsening trend of point-bar deposits

Many previous studies of fluvial point-bar successions have proposed generalised point-bar facies models that depict an overall fining-upward trend as a result of helicoidal flow in the meander bend (Allen, 1963). Thus, the fining-upward succession in point-bars is a widely occurring and much-documented phenomenon (e.g., Allen, 1963; Miall, 1996; Ghazi and Mountney, 2009). However, studies of some point-bar deposits have revealed coarsening-upward grain-size trends in other meandering river systems (e.g., McGowen and Garner, 1970; Bluck, 1971; Jackson, 1976; Ghinassi et al., 2013; Słowik, 2016). These meandering river systems are noted in humid and temperate regions. Additionally, the point-bar deposits are mainly fine sand and coarse sand ( $D_{50} > 250 \mu\text{m}$ ), some gravelly, and deposits overall are indicative of high-energy flow conditions. This study reveals that in the non-vegetated ephemeral Río Colorado river terminus, point-bar deposits (both in the presently active channel and in abandoned palaeo-channels) can be characterised by a coarsening-upward succession with very fine-grained deposits at the base and an increasing proportion of coarser sediments toward the top (Fig. 10).

Since topographic changes due to tectonics can be discounted for the short evolutionary time periods considered here (Bills et al., 1994), it is concluded that the topography (landscape) of the terminus system of the Río Colorado investigated here remained essentially constant. It is also unlikely that the sediment supply from the source area had dramatically changed during this period. Additionally, the Río Colorado terminus system traverses an extremely low-gradient former lake bottom with no appreciable topography on the floodplain (Donselaar et al., 2013; Li et al., 2015, 2019). Multi-decadal Landsat imagery (1985–2011) has revealed that the Río Colorado terminus has remained a near-constant size in recent decades, with a mean area of 419 km<sup>2</sup> and standard deviation of 21 km<sup>2</sup> (Li et al., 2014b). Through analysis of field-acquired data and laboratory testing data, the following key observations regarding the sedimentology of the point-bar deposits in the Río Colorado terminus are made: 1) experiments demonstrate that fine sediment size fractions can be transported as individual particles in the river system such that granulometric analysis using a laser particle sizer is appropriate; 2) point-bar deposits along channel C2 and C0 are characterised by coarsening-upward vertical sedimentary successions;

and 3) the coarsening-upward succession in the distal part of the river terminus can be shown to be related to sedimentation during an episode of an overall increasing trend in the maximum daily precipitation over a decadal period (2005 to 2016).

Therefore, we propose a novel point-bar model whereby lateral accretion sediment packages record the spatial and temporal development of meander point-bars (Fig. 13). Various accretion layers represent different periods of major peak floods and the accretion layers away from the channel are chronologically older than those close to the channel (Nanson, 1980). The sediment supply of the various grain-size classes for different periods is constrained by floodwater flow power and duration, meaning that different magnitudes and durations of floods (indicative of wetness) imply variations in the sediment transport capacity of the river (Ferguson, 1987; Alexandrov et al., 2003). Therefore, it may be supposed that during episodes of low-magnitude, short-duration flooding, only fine sediment can be transported downstream due to reduced stream power; such sediments might ultimately be deposited from suspension fallout in standing water. By contrast, high-magnitude, longer-duration flood events are likely to be able to transport increasingly coarse-grained sediment further downstream in the system (e.g., Graf, 1988; Alexandrov et al., 2003). Given the ephemeral nature of the flow and the gradual lateral migration of meandering channels in the low-gradient river termini, gently inclined slopes of accretion layers lead to the accumulation of coarse deposits that overlie deposits in response to an overall trend of successive flood events with increasing magnitude and duration.

One alternative potential mechanism for point-bar evolution would be the development of fining-upward point-bar successions via the “traditional model”, whereby coarsest deposits accumulated in the channel thalweg, and successively finer deposits accumulate on higher parts of the inner bend of a meander (Allen, 1963; Ghazi and Mountney, 2009; Collinson and Mountney, 2019). Yet, exceptions to this model are noted in the dataset from this study; the grain-size distribution data and the end-member modelling reveal vertical coarsening-upward successions in several of the studied point bars.

A second alternative potential mechanism by which a coarsening upward point-bar succession could develop is via the gradual evolution a long-lived point bar that commences its growth at the very distal terminus of the river where only the finest sediment fractions reach (Nichols and Fisher, 2007; North and Davidson, 2012). The distal river terminus might then gradually prograde forwards across the dry lakebed during the lifecycle of the point bar such that slightly coarser sediment fractions might accumulate in the upper parts of the point bar. The ongoing progradation of the river terminus across the dry lakebed provides the mechanism to accumulate a coarsening upward succession. However, such a coarsening-upward point-bar succession would be expected to develop both in the proximal and distal terminus for a channel (C2) in the Río Colorado terminus.

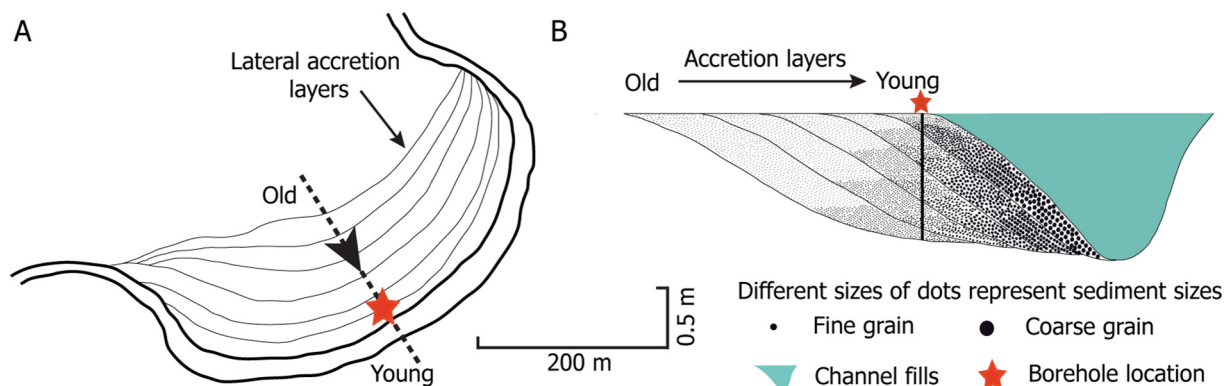


Fig. 13. Schematic diagram illustrating a coarsening-upward sequence of a point bar.

The favoured proposed model best matches the observations from the Río Colorado. Besides the laboratory analysis and field observations, in the literature, palaeolimnological studies revealed that between 1 cal. ka and 0.5 cal. ka a notably dry climate dominated after which there was a switch to a trend of increasing wetness in the Andes. This is revealed through multiple proxies (palynological and isotopic studies) (Valero-Garcés et al., 1996; Abbott et al., 1997; Mourguiart et al., 1998; Sublette Mosblech et al., 2012). These observations additionally support the proposed conceptual model that lateral accretion layers of point-bar deposits, with inherent variability in sediment characteristics, are a function of river dynamics, especially those relating to changes in the durations and magnitudes of ephemeral river flows. However, to further validate the relationship, long-term hydrological data and corresponding sedimentation data are required for future studies.

## 7. Conclusions

A coarsening-upward succession in the fine-grained Río Colorado terminus of an endorheic basin in Salar de Uyuni has been examined. The succession, which records point-bar deposits, has been examined using GSD (with EMMA) and mineralogical analyses (XRD and LOI). Analyses of GSD and EMMA revealed a common upward-coarsening trend for numerous point-bar deposits in terms of  $D_{50}$  of GSD and proportions of coarse sediment for two (C2 and C0) of three chronologically different meandering channels in the river terminus. Those of another abandoned channel (C1) were dominated by fining-upward deposits. Channel C2, which is dominated by a coarsening-upward succession of point-bar deposits, was also characterised by a lower content of organic matter and carbonate compared with the other two studied channels. A conceptual model to account for the coarsening-upward successions of point-bar deposits has been established. The coarsening-upward sequence likely arose in response to low-frequency, high-magnitude floods at the beginning of a sedimentary cycle during a hyper-arid period when the sediment supply to the river terminus was clay or fine silt dominated. A temporal trend toward higher magnitude and longer duration flood events enables the transport of coarser-grained sediments further down system toward the river terminus where deposition occurs on the inner bend of meandering channels. Successive accretion layers within the point-bar deposits record a coarsening upward trend, which likely reflects this temporal trend. The apparently common occurrence of coarsening-upward succession for numerous point-bar deposits in a muddy river terminus of a semi-arid endorheic basin not only explains the sedimentary architecture model of such depositional environment but may also indicate the associated palaeohydrology.

## Declaration of competing interest

The authors declare that they have no known competing financial interests or personal relationships that could have appeared to influence the work reported in this paper.

## Acknowledgements

Analyses of grain-size distribution and LOI were performed at the VU University Amsterdam. JL thanks C.S. Bristow and M.A. Prins for constructive preliminary discussions. Help of Michael Dietze is appreciated for his support on the EMMA analysis. This research was supported by the National Natural Science Foundation of China (No. 41602121 and 41972114), and the Fundamental Research Funds for the Central Universities, China University of Geosciences, Wuhan (No. CUG150616) and Open Fund (TPR-2017-01) of Key Laboratory (Ministry of Education) of Tectonics and Petroleum Resources (China University of Geosciences, Wuhan, China). We are grateful for constructive comments from Editor Catherine Chagué and from two anonymous reviewers, which have improved this manuscript.

## References

- Abbott, M.B., Seltzer, G.O., Kelts, K.R., Southon, J., 1997. Holocene paleohydrology of the tropical Andes from lake records. *Quat. Res.* 47, 70–80.
- Alexandrov, Y., Laronne, J.B., Reid, I., 2003. Suspended sediment concentration and its variation with water discharge in a dryland ephemeral channel, northern Negev, Israel. *J. Arid Environ.* 53, 73–84.
- Allen, J.R.L., 1963. The classification of cross-stratified units with notes on their origin. *Sedimentology* 2, 93–114.
- Argollo, J., Mourguiart, P., 2000. Late Quaternary climate history of the Bolivian Altiplano. *Quat. Int.* 72, 37–51.
- Baker, P.A., Rigsby, C.A., Seltzer, G.O., Fritz, S.C., Lowenstein, T.K., Bacher, N.P., Veliz, C., 2001. Tropical climate changes at millennial and orbital timescales on the Bolivian Altiplano. *Nature* 409, 698–701.
- Baucom, P.C., Rigsby, C.A., 1999. Climate and lake-level history of the northern Altiplano, Bolivia, as recorded in Holocene sediments of the Rio Desaguadero. *J. Sediment. Res.* 69, 597–611.
- Bills, B.G., de Silva, S.L., Currey, D.R., Emenger, R.S., Lillquist, K.D., Donnellan, A., Worden, B., 1994. Hydro-isostatic deflection and tectonic tilting in the central Andes: initial results of a GPS survey of Lake Minchin shorelines. *Geophys. Res. Lett.* 21, 293–296.
- Bluck, B.J., 1971. Sedimentation in the meandering river Endrick. *Scott. J. Geol.* 7, 93–138.
- Bridge, J.S., Alexander, J., Collier, R.E.L., Gawthorpe, R.L., Jarvis, J., 1995. Ground-penetrating radar and coring used to study the large-scale structure of point-bar deposits in three dimensions. *Sedimentology* 42, 839–852.
- Camacho Suarez, V.V., Saraiva Okello, A.M.L., Weninger, J.W., Uhlenbrook, S., 2015. Understanding runoff processes in a semi-arid environment through isotope and hydrochemical hydrograph separations. *Hydrol. Earth Syst. Sci.* 19, 4183–4199.
- Collinson, J.C., Mountney, N.P., 2019. *Sedimentary Structures*. fourth edition. Dunedin Academic Press, Edinburgh 978-1780460628 (340 pp.).
- Colombera, L., Mountney, N.P., 2019. The lithofacies organization of fluvial channel deposits: a meta-analysis of modern rivers. *Sediment. Geol.* 383, 16–40.
- Colombera, L., Mountney, N.P., McCaffrey, W.D., 2013. A quantitative approach to fluvial facies models: methods and example results. *Sedimentology* 60, 1526–1558.
- Comiti, F., Da Canal, M., Surian, N., Mao, L., Picco, L., Lenzi, M.A., 2011. Channel adjustments and vegetation cover dynamics in a large gravel bed river over the last 200 years. *Geomorphology* 125, 147–159.
- Coronel, M.D., Isla, M.F., Veiga, G.D., Mountney, N.P., Colombera, L., 2020. Anatomy and facies distribution of terminal lobes in ephemeral fluvial successions: Jurassic Tordillo Formation, Neuquén Basin, Argentina. *Sedimentology* <https://doi.org/10.1111/sed.12712>.
- Dietze, M., Dietze, E., 2013. EMMAgeo: end-member modelling algorithm and supporting functions for grain-size analysis. R package version 0.9.1. <http://CRAN.R-project.org/package=EMMAgeo>.
- Dietze, E., Hartmann, K., Diekmann, B., Ijmker, J., Lehmkühl, F., Opitz, S., Stauch, G., Wünnemann, B., Borchers, A., 2012. An end-member algorithm for deciphering modern detrital processes from lake sediments of Lake Donggi Cona, NE Tibetan Plateau, China. *Sediment. Geol.* 243–244, 169–180.
- Dietze, E., Maussion, F., Ahlborn, M., Diekmann, B., Hartmann, K., Henkel, K., Kasper, T., Lockot, G., Opitz, S., Haberzettl, T., 2014. Sediment transport processes across the Tibetan Plateau inferred from robust grain-size end members in lake sediments. *Clim. Past* 10, 91–106.
- Dietze, M., Dietze, E., Lomax, J., Fuchs, M., Kleber, A., Wells, S.G., 2016. Environmental history recorded in aeolian deposits under stone pavements, Mojave Desert, USA. *Quat. Res.* 85, 4–16.
- Donselaar, M.E., Gozalo, M.C.C., Moyano, S., 2013. Avulsion processes at the terminus of low-gradient semi-arid fluvial systems: lessons from the Río Colorado, Altiplano endorheic basin, Bolivia. *Sediment. Geol.* 283, 1–14.
- Donselaar, M.E., Bhatt, A.G., Ghosh, A.K., 2017a. On the relation between fluvio-deltaic flood basin geomorphology and the wide-spread occurrence of arsenic pollution in shallow aquifers. *Sci. Total Environ.* 574, 901–913.
- Donselaar, M.E., Cuevas Gozalo, M.C., Wallinga, J., 2017b. Avulsion history of a Holocene semi-arid river system - outcrop analogue for thin-bedded fluvial reservoirs in the Rotliegend feather edge. 79th EAGE Conference and Exhibition 2017. EAGE, Paris, pp. 12–15.
- Elger, K., Oncken, O., Glodny, J., 2005. Plateau-style accumulation of deformation: Southern Altiplano. *Tectonics* 24. <https://doi.org/10.1029/2004TC001675>.
- Ferguson, R.I., 1987. Accuracy and precision of methods for estimating river loads. *Earth Surf. Process. Landf.* 12, 95–104.
- Ferguson, R.I., Hoey, T., Wathen, S., Werritty, A., 1996. Field evidence for rapid downstream fining of river gravels through selective transport. *Geology* 24, 179–182.
- Frings, R.M., 2008. Downstream fining in large sand-bed rivers. *Earth Sci. Rev.* 87, 39–60.
- Ghazi, S., Mountney, N.P., 2009. Facies and architectural element analysis of a meandering fluvial succession: the Permian Warchha Sandstone, Salt Range, Pakistan. *Sediment. Geol.* 221, 99–126.
- Ghinassi, M., Billi, P., Libsekal, Y., Papini, M., Rook, L., 2013. Inferring fluvial morphodynamics and overbank flow control from 3D outcrop sections of a Pleistocene point bar, Dandiero Basin, Eritrea. *J. Sediment. Res.* 83, 1065–1083.
- Gibling, M.R., Nanson, G.C., Maroulis, J.C., 1998. Anastomosing river sedimentation in the Channel Country of central Australia. *Sedimentology* 45, 595–619.
- Graf, W.L., 1988. *Fluvial Processes in Dryland Rivers*. Springer-Verlag, Berlin, p. 346.
- Grosjean, M., 1994. Paleohydrology of the Laguna Lejía (north Chilean Altiplano) and climatic implications for late-glacial times. *Palaeogeogr. Palaeoclimatol. Palaeoecol.* 109, 89–100.
- Heiri, O., Lotter, A.F., Lemcke, G., 2001. Loss on ignition as a method for estimating organic and carbonate content in sediments: reproducibility and comparability of results. *J. Paleolimnol.* 25, 101–110.

- Horton, B.K., Hampton, B.A., Waanders, G.L., 2001. Paleogene synorogenic sedimentation in the Altiplano plateau and implications for initial mountain building in the central Andes. *GSA Bull.* 113, 1387–1400.
- Ielipi, A., 2018. Morphodynamics of meandering streams devoid of plant life: Amargosa River, Death Valley, California. *GSA Bull.* 131, 782–802.
- Ielipi, A., Ghinassi, M., Rainbird, R.H., Ventra, D., 2019. Planform sinuosity of Proterozoic rivers: a craton to channel-reach perspective. In: Ghinassi, M., Colomera, L., Mountney, N.P., Reesink, A.J.H. (Eds.), *Fluvial Meanders and Their Sedimentary Products in the Rock Record*. International Association of Sedimentologists Special Publication 48, pp. 81–118.
- Jackson II, R.G., 1976. Depositional model of point bars in the Lower Wabash River. *J. Sediment. Petrol.* 46, 579–594.
- Jackson II, R.G., 1981. Sedimentology of muddy fine-grained channel deposits in meandering streams of the American middle west. *J. Sediment. Res.* 51, 1169–1192.
- Kemp, J., 2010. Downstream channel changes on a contracting, anabranching river: the Lachlan, southeastern Australia. *Geomorphology* 121, 231–244.
- Knighton, A.D., 1980. Longitudinal changes in size and sorting of stream-bed material in four English rivers. *GSA Bull.* 91, 55–62.
- Knighton, A.D., Nanson, G.C., 2001. An event-based approach to the hydrology of arid zone rivers in the channel country of Australia. *J. Hydrol.* 254, 102–123.
- Konert, M., Vandenberghe, J., 1997. Comparison of laser grain size analysis with pipette and sieve analysis: a solution for the underestimation of the clay fraction. *Sedimentology* 44, 523–535.
- Lamparelli, R.A.C., Ponzoni, F.J., Zullo, J., Pellegrino, G.Q., Arnaud, Y., 2003. Characterization of the Salar de Uyuni for in-orbit satellite calibration. *IEEE Trans. Geosci. Remote Sens.* 41, 1461–1468.
- Li, J., 2014. Terminal fluvial systems in a semi-arid endorheic basin, Salar de Uyuni (Bolivia). *Uitgeverij BOX Press, 's-Hertogenbosch*. The Netherlands, p. 10.
- Li, J., Bristow, C.S., 2015. Crevasse splay morphodynamics in a dryland river terminus: Río Colorado in Salar de Uyuni Bolivia. *Quat. Int.* 377, 71–82.
- Li, J., Donselaar, M.E., Hosseini Aria, S.E., Koenders, R., Oyen, A.M., 2014a. Landsat imagery-based visualization of the geomorphological development at the terminus of a dryland river system. *Quat. Int.* 352, 100–110.
- Li, J., Menenti, M., Mousivand, A., Luthi, S.M., 2014b. Non-vegetated playa morphodynamics using multi-temporal landsat imagery in a semi-arid endorheic basin: Salar de Uyuni, Bolivia. *Remote Sens.* 6, 10131–10151.
- Li, J., Luthi, S.M., Donselaar, M.E., Weltje, G.J., Prins, M.A., Bloemsa, M.R., 2015. An ephemeral meandering river system: sediment dispersal processes in the Río Colorado, Southern Altiplano Plateau, Bolivia. *Z. Geomorphol.* 59, 301–317.
- Li, J., Yang, X., Maffei, C., Tooth, S., Yao, G., 2018. Applying independent component analysis on Sentinel-2 imagery to characterize geomorphological responses to an extreme flood event near the non-vegetated Río Colorado terminus, Salar de Uyuni, Bolivia. *Remote Sens.* 10, 725. <https://doi.org/10.3390/rs10050725>.
- Li, J., Tooth, S., Yao, G., 2019. Cascades of sub-decadal, channel-floodplain changes in low-gradient, non-vegetated reaches near a dryland river terminus: Salar de Uyuni, Bolivia. *Earth Surf. Process. Landf.* 44, 490–506.
- Li, J., Grenfell, M.C., Wei, H., Tooth, S., Ngium, S., 2020. Chute cutoff-driven abandonment and sedimentation of meander bends along a fine-grained, non-vegetated, ephemeral river on the Bolivian Altiplano. *Geomorphology* 350, 106917. <https://doi.org/10.1016/j.geomorph.2019.106917>.
- Marconato, A., de Almeida, R.P., Turra, B.B., dos Fragoso-Cesar, A.Ó.R.S., 2014. Pre-vegetation fluvial floodplains and channel-belts in the Late Neoproterozoic-Cambrian Santa Bárbara group (Southern Brazil). *Sediment. Geol.* 300, 49–61.
- Marouli, J.C., Nanson, G.C., 1996. Bedload transport of aggregated muddy alluvium from Cooper Creek, central Australia: a flume study. *Sedimentology* 43, 771–790.
- Marren, P.M., McCarthy, T.S., Tooth, S., Brandt, D., Stacey, G.G., Leong, A., Spottiswoode, B., 2006. A comparison of mud- and sand-dominated meanders in a downstream coarsening reach of the mixed bedrock-alluvial Klip River, eastern Free State, South Africa. *Sediment. Geol.* 190, 213–226.
- McGowen, J.H., Garner, L.E., 1970. Physiographic features and stratification types of coarse-grained point bars: modern and ancient examples. *Sedimentology* 14, 77–111.
- McMahon, W.J., Davies, N.S., 2018. The shortage of geological evidence for pre-vegetation meandering rivers. In: Ghinassi, M., Colomera, L., Mountney, N.P., Reesink, A.J.H. (Eds.), *Fluvial Meanders and Their Sedimentary Products in the Rock Record*. International Association of Sedimentologists Special Publication 48, pp. 119–148.
- Miall, A.D., 1988. Reservoir heterogeneities in fluvial sandstones: lessons from outcrop studies. *Am. Assoc. Pet. Geol. Bull.* 72, 682–697.
- Miall, A.D., 1996. *The Geology of Fluvial Deposits: Sedimentary Facies, Basin Analysis, and Petroleum Geology*. Springer-Verlag, New York (582 pp.).
- Micheli, E.R., Kirchner, J.W., 2002. Effects of wet meadow riparian vegetation on streambank erosion. 1. Remote sensing measurements of streambank migration and erodibility. *Earth Surf. Process. Landf.* 27, 627–639.
- Mourguiart, P., Correge, T., Wirmann, D., Argollo, J., Montenegro, M.E., Pourchet, M., Carbonel, P., 1998. Holocene paleoclimatology of Lake Titicaca estimated from an ostracod-based transfer function. *Palaeogeogr. Palaeoclimatol. Palaeoecol.* 143, 51–72.
- Müller, R., Nystuen, J.P., Wright, V.P., 2004. Pedogenic mud aggregates and paleosol development in ancient dryland river systems: criteria for interpreting alluvial mudrock origin and floodplain dynamics. *J. Sediment. Res.* 74, 537–551.
- Nanson, G.C., 1980. Point bar and floodplain formation of the meandering Beaton River, northeastern British Columbia, Canada. *Sedimentology* 27, 3–29.
- Nanson, G.C., Tooth, S., Knighton, A.D., 2002. A global perspective on dryland rivers: perceptions, misconceptions and distinctions. In: Bull, L.J., Kirkby, M.J. (Eds.), *Dryland Rivers*. Wiley, Chichester, pp. 17–54.
- Nichols, G.J., Fisher, J.A., 2007. Processes, facies and architecture of fluvial distributary system deposits. *Sediment. Geol.* 195, 75–90.
- North, C.P., Davidson, S.K., 2012. Unconfined alluvial flow processes: recognition and interpretation of their deposits, and the significance for palaeogeographic reconstruction. *Earth Sci. Rev.* 111, 199–223.
- Page, K.J., Nanson, G.C., Frazier, P.S., 2003. Floodplain formation and sediment stratigraphy resulting from oblique accretion on the Murrumbidgee River, Australia. *J. Sediment. Res.* 73, 5–14.
- Placzek, C., Quade, J., Patchett, P.J., 2006. Geochronology and stratigraphy of late Pleistocene lake cycles on the southern Bolivian Altiplano: implications for causes of tropical climate change. *GSA Bull.* 118, 515–532.
- Placzek, C.J., Quade, J., Patchett, P.J., 2011. Isotopic tracers of paleohydrologic change in large lakes of the Bolivian Altiplano. *Quat. Res.* 75, 231–244.
- Prins, M.A., Weltje, G.J., 1999. End-member modeling of siliciclastic grain-size distributions: the late Quaternary record of eolian and fluvial sediment supply to the Arabian Sea and its paleoclimatic significance. In: Harbaugh, J., Watney, L., Rankey, G. (Eds.), *Numerical Experiments in Stratigraphy: Recent Advances in Stratigraphic and Sedimentologic Computer Simulations*. SEPM Special Publication, Society for Sedimentary Geology 62, pp. 91–111.
- Prins, M.A., Postma, G., Weltje, G.J., 2000. Controls on terrigenous sediment supply to the Arabian Sea during the late Quaternary: the Makran continental slope. *Mar. Geol.* 169, 327–349.
- Rice, S., Church, M., 1998. Grain size along two gravel-bed rivers: statistical variation, spatial pattern and sedimentary links. *Earth Surf. Process. Landf.* 23, 345–363.
- Rigsby, C.A., Bradbury, J.P., Baker, P.A., Rollins, S.M., Warren, M.R., 2005. Late Quaternary palaeolakes, rivers, and wetlands on the Bolivian Altiplano and their palaeoclimatic implications. *J. Quat. Sci.* 20, 671–691.
- Risacher, F., Fritz, A.B., Lerman, A., 2009. Origin of salts and brine evolution of Bolivian and Chilean salars. *Aquat. Geochem.* 15, 123–157.
- Rust, B.R., Nanson, G.C., 1989. Bedload transport of mud as pedogenic aggregates in modern and ancient rivers. *Sedimentology* 36, 291–306.
- Rygel, M.C., Gibling, M.R., 2006. Natural geomorphic variability recorded in a high-accommodation setting: fluvial architecture of the Pennsylvanian Joggins Formation of Atlantic Canada. *J. Sediment. Res.* 76, 1230–1251.
- Sambrook Smith, G.H., Best, J.L., Leroy, J.Z., Orfeo, O., 2016. The alluvial architecture of a suspended sediment dominated meandering river: the Río Bermejo, Argentina. *Sedimentology* 63, 1187–1208.
- Santos, M.G.M., Mountney, N.P., Peakall, J., 2017. Tectonic and environmental controls on palaeozoic fluvial environments: reassessing the impacts of early land plants on sedimentation. *J. Geol. Soc. Lond.* 174, 393–404.
- Santos, M.G.M., Hartley, A.J., Mountney, N.P., Peakall, J., Owen, A., Merino, E.R., Assine, M.L., 2019. Meandering rivers in modern desert basins: implications for channel planform controls and prevegetation rivers. *Sediment. Geol.* 385, 1–14.
- Shiers, M.N., Mountney, N.P., Hodgson, D.M., Colomera, L., 2019. Controls on the depositional architecture of fluvial point-bar elements in a coastal-plain succession. In: Ghinassi, M., Colomera, L., Mountney, N.P., Reesink, A.J.H. (Eds.), *Fluvial Meanders and Their Sedimentary Products in the Rock Record*. International Association of Sedimentologists Special Publication 48, pp. 15–46.
- Simon, S.S.T., Gibling, M.R., 2017a. Fine-grained meandering systems of the Lower Permian Clear Fork Formation of north-central Texas, USA: lateral and oblique accretion on an arid plain. *Sedimentology* 64, 714–746.
- Simon, S.S.T., Gibling, M.R., 2017b. Pedogenic mud aggregates preserved in a fine-grained meandering channel in the Lower Permian Clear Fork Formation, north-central Texas, USA. *J. Sediment. Res.* 87, 230–252.
- Slingerland, R., Smith, N.D., 2004. River avulsion and their deposits. *Annu. Rev. Earth Planet. Sci.* 32, 257–285.
- Ślowik, M., 2016. Sedimentary record of point bar formation in laterally migrating anabranching and single-channel meandering rivers (The Obra Valley, Poland). *Z. Geomorphol.* 60, 259–279.
- Ślowik, M., Dezső, J., Kovács, J., Gałka, M., 2020. The formation of low-energy meanders in loess landscapes (Transdanubia, central Europe). *Glob. Planet. Chang.* 184, 103071. <https://doi.org/10.1016/j.gloplacha.2019.103071>.
- Smith, D.G., Hubbard, S.M., Leckie, D.A., Fustic, M., 2009. Counter point bar deposits: lithofacies and reservoir significance in the meandering modern peace river and ancient McMurray formation, Alberta, Canada. *Sedimentology* 56, 1655–1669.
- Straub, K.M., Paola, C., Mohrig, D., Wolinsky, M.A., George, T., 2009. Compensational stacking of channelized sedimentary deposits. *J. Sediment. Res.* 79, 673–688.
- Sublette Mosblech, N.A., Chepstow-Lusty, A., Valencia, B.G., Bush, M.B., 2012. Anthropogenic control of late-Holocene landscapes in the Cuzco region, Peru. *The Holocene* 22, 1361–1372.
- Sun, Y., Lu, H., An, Z., 2006. Grain size of loess, palaeosol and Red Clay deposits on the Chinese Loess Plateau: significance for understanding pedogenic alteration and palaeomonsoon evolution. *Palaeogeogr. Palaeoclimatol. Palaeoecol.* 241, 129–138.
- Sun, D., Su, R., Li, Z., Lu, H., 2011. The ultrafine component in Chinese loess and its variation over the past 7.6Ma: implications for the history of pedogenesis. *Sedimentology* 58, 916–935.
- Sylvestre, F., Servant-Vildary, S., Fournier, M., Servant, M., 1995. Lake levels in the southern Bolivian Altiplano (19°–21°S.) during the Late Glacial based on diatom studies. *Int. J. Salt Lake Res.* 4, 281–300.
- Thomas, R.G., Smith, D.G., Wood, J.M., Visser, J., Calverley-range, E.A., Koster, E.H., 1987. Inclined heterolithic stratification—terminology, description, interpretation and significance. *Sediment. Geol.* 53, 123–179.
- Tooth, S., 2000. Process, form and change in dry land rivers: a review of recent research. *Earth Sci. Rev.* 51, 67–107.
- Valero-Garcés, B., Grosjean, M., Schwab, A., Geyh, M., Messerli, B., Kelts, K., 1996. Limnogeology of Laguna Miscanti: evidence for mid to late Holocene moisture changes in the Atacama Altiplano (Northern Chile). *J. Paleolimnol.* 16, 1–21.

- van Toorenburg, K.A., Donselaar, M.E., Weltje, G.J., 2018. The life cycle of crevasse splays as a key mechanism in the aggradation of alluvial ridges and river avulsion. *Earth Surf. Process. Landf.* 43, 2409–2420.
- Vandenberghe, J., 2013. Grain size of fine-grained windblown sediment: a powerful proxy for process identification. *Earth Sci. Rev.* 121, 18–30.
- Vandenberghe, J., Gracheva, R., Sorokin, A., 2010. Postglacial floodplain development and Mesolithic-Neolithic occupation in the Russian forest zone. *Proc. Geol. Assoc.* 121, 229–237.
- Vandenberghe, J., de Moor, J.J.W., Spanjaard, G., 2012. Natural change and human impact in a present-day fluvial catchment: the Geul River, Southern Netherlands. *Geomorphology* 159–160, 1–14.
- Vandenberghe, J., Sun, Y., Wang, X., Abels, H.A., Liu, X., 2018. Grain-size characterization of reworked fine-grained aeolian deposits. *Earth Sci. Rev.* 177, 43–52.
- Visher, G.S., 1964. Fluvial processes as interpreted from ancient and recent fluvial deposits. *Am. Assoc. Pet. Geol. Bull.* 48, 550.
- Wakelin-King, G.A., Webb, J.A., 2007. Threshold-dominated fluvial styles in an arid-zone mud-aggregate river: the uplands of Fowlers Creek, Australia. *Geomorphology* 85, 114–127.
- Wang, C., Adriaens, R., Hong, H., Elsen, J., Vandenberghe, N., Lourens, L.J., Gingerich, P.D., Abels, H.A., 2017. Clay mineralogical constraints on weathering in response to early Eocene hyperthermal events in the Bighorn Basin, Wyoming (Western Interior, USA). *GSA Bull.* 129, 997–1011.
- Weltje, G.J., 1997. End-member modeling of compositional data: numerical-statistical algorithms for solving the explicit mixing problem. *Math. Geol.* 29, 503–549.
- Wright, V.P., Marriott, S.B., 2007. The dangers of taking mud for granted: lessons from Lower Old Red Sandstone dryland river systems of South Wales. *Sediment. Geol.* 195, 91–100.
- Yan, N., Mountney, N.P., Colombera, L., Dorrell, R.M., 2017. A 3D forward stratigraphic model of fluvial meander-bend evolution for prediction of point-bar lithofacies architecture. *Comput. Geosci.* 105, 65–80.
- Zeeden, C., Kels, H., Hambach, U., Schulte, P., Protze, J., Eckmeier, E., Marković, S.B., Klasen, N., Lehmkuhl, F., 2016. Three climatic cycles recorded in a loess-palaeosol sequence at Semic (Romania) – implications for dust accumulation in south-eastern Europe. *Quat. Sci. Rev.* 154, 130–142.